FISEVIER

Contents lists available at ScienceDirect

Journal of Hydrology

journal homepage: www.elsevier.com/locate/jhydrol

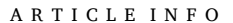


Research papers

Climatic and anthropogenic controls on groundwater dynamics in the Mekong River Basin

Tamanna Kabir^a, Yadu Pokhrel^{a,*}, Farshid Felfelani^{a,b}

- ^a Department of Civil and Environmental Engineering, Michigan State University, East Lansing, MI, USA
- ^b Research Applications Lab, The University Corporation for Atmospheric Research, Boulder, CO, USA



This manuscript was handled by Marco Borga, Editor-in-Chief, with the assistance of Christian Massari, Associate Editor

Keywords: Mekong River Basin Groundwater dynamics Community Land Model Irrigation Groundwater pumping

ABSTRACT

Groundwater depletion is a worldwide concern and an emerging issue in regions such as the Mekong River Basin (MRB). However, even the natural dynamics of groundwater in the MRB is yet to be fully explored, making the quantification of groundwater response to climate variability and anthropogenic activities a major scientific challenge. Here, we examine various groundwater mechanisms in the MRB, focusing on groundwater flow processes that are modulated by climate variability, physiographic features, and key drivers of groundwatersurface water interactions. We further quantify the influence of anthropogenic activities on groundwater dynamics. We use the Community Land Model version 5 (CLM5) at 0.05° (~5km) spatial resolution with an improved representation of groundwater processes, including lateral groundwater flow and aquifer pumping for irrigation. Results indicate high spatial heterogeneity in groundwater recharge and discharge across the basin governed by climate and subsurface characteristics. A pronounced seasonality is found in groundwater recharge due to precipitation; ~52% of wet season precipitation recharges groundwater, with substantial carryover to the consecutive dry season that alleviates soil moisture. Importantly, groundwater discharge is a dominant source of streamflow all year round, which suggests a strong surface water-groundwater coupling in the MRB. Finally, our results indicate that irrigation pumping is directly altering groundwater flows and storages; climate variability smoothens pumping effects over long times, but the model simulates region-wide groundwater depletion (up to 1 m/year) in the Mekong Delta during dry years. Our study provides key insights on the evolving groundwater systems in the MRB, also advancing process-based groundwater modeling capabilities.

1. Introduction

Groundwater is a crucial component of the global water cycle (Condon et al., 2021; Cooper, 2010; Ferguson and Maxwell, 2010; Miguez-Macho and Fan, 2012a). It is the world's largest freshwater resource that supplies water to billions of people, forms an integral part of irrigated agriculture, and contributes to the health of many ecosystems (Siebert & Döll, 2010, Cuthbert et al., 2019; Gleeson et al., 2012). At least one-fourth of the world's population heavily relies on groundwater (Döll, 2009). The dependence will likely continue to grow in the future due to the increase in population and associated demands for water, especially agricultural (Siebert & Döll, 2010, Siebert et al., 2015). Agricultural irrigation—which accounts for over 70% of the total freshwater withdrawal and 90% of the consumptive water use (Gleick, 2018; Shiklomanov, 2000)—is reliant heavily on groundwater in many global regions, especially those with limited surface water (Hanasaki

et al., 2013; Leng et al., 2014; Reinecke et al., 2021; Wada et al., 2013). This reliance is expected to rise sharply owing to increased irrigation needs in relatively dry agricultural regions (Ambika and Mishra, 2019; Crosbie et al., 2013; Scanlon et al., 2012; Wada et al., 2013) or even in relatively humid regions such as the Mekong River Basin (MRB) that are experiencing rapid agricultural intensification (Hoang et al., 2019; Nguyen et al., 2012; Sakamoto et al., 2009) or increased groundwater pumping as surface water availability continues to decline (Erban and Gorelick, 2016; Minderhoud et al., 2017). Therefore, there is a growing need, as well as an interest, to improve our understanding of groundwater processes, especially through process-based modeling; however, major challenges remain due to the complexity of groundwater system (Cuthbert et al., 2019; Fan et al., 2019, 2007; Gleeson et al., 2016).

Groundwater dynamics is modulated by a variety of regional to local hydrological processes that are intricately interconnected and governed by climatic drivers, topographic controls, and hydrogeological

E-mail address: ypokhrel@msu.edu (Y. Pokhrel).

^{*} Corresponding author.

characteristics (Cuthbert et al., 2019). Thus, groundwater research poses unique challenges compared to the study of surface water and it is exceedingly difficult to assess and predict the changes in groundwater systems, especially over large scales (Condon & Maxwell, 2015; Engdahl, 2017; Sophocleous, 2002). Observational data challenges make groundwater research even more daunting (Evans et al., 2020; Megdal et al., 2015), which is particularly true for modeling studies that require such data both to constrain and validate the models. Especially in datalimited regions, even selecting an appropriate model can be challenging (Kumar et al., 2021; Tegegne et al., 2017). Parsimonious models are often used in such regions because of their simplicity and limited data requirements (Pande et al., 2012; Quichimbo et al., 2021). However, while parsimonious models could realistically simulate certain hydrologic variables under constrained conditions, the models are not well suited to study process interactions and the complexities therein (e.g., land use change, vegetation processes, soil hydrology) (Fenicia et al., 2011; Wu et al., 2010), especially considering that a system response to changing climatic and human drivers can be non-linear (Mcguire and Mcdonnell, 2010; Sivapalan et al., 2002).

Conversely, process-based models (e.g., land surface models; LSMs), offer a more physically-based representation of surface and subsurface hydrological processes, including infiltration, soil moisture dynamics, and groundwater recharge, making these models more robust and feasible for application in different regions and climates, especially in data-limited basins such as the MRB (Koirala et al., 2014; Pokhrel et al., 2014; de Graaf et al., 2015; Gleeson et al., 2021). Furthermore, LSMs offer promising avenues for future research on land–atmosphere coupling, enabling an improved understanding of the dynamic interactions between groundwater and the atmosphere, and more broadly within the entire Earth system (Clark et al., 2015). As such, many large-scale groundwater modeling studies use LSMs account for groundwater in a relatively simple manner or with minimal groundwater parametrizations (Koirala et al., 2019; Pokhrel et al., 2016).

Despite the challenges in representing groundwater in LSMs due to data scarcity, among others, notable progress has been made toward improved groundwater parameterizations. Some of the noteworthy advances include the representation of linear groundwater reservoir (Fenicia et al., 2006), surface water-groundwater interactions (Fan and Schaller, 2009; Kollet and Maxwell, 2008; Maxwell and Kollet, 2008; Miguez-Macho and Fan, 2012a, 2012b), lateral groundwater flow (Barlage et al., 2021; de Graaf and Stahl, 2022; Felfelani et al., 2021; Zeng et al., 2018), and groundwater pumping for irrigation (de Graaf et al., 2019; Felfelani et al., 2021; Leng et al., 2014; Nie et al., 2018; Pokhrel et al., 2012, 2015; Wada et al., 2010). These efforts have led to groundwater representations with varying degree of complexity in different LSMs including the Variable Infiltration Capacity Model (VIC) (Liang et al., 2003), MATSIRO (Pokhrel et al., 2015), Community Land Model (CLM) (Kluzek, 2013; Lawrence et al., 2019; Oleson et al., 2013; Swenson et al., 2019), and Noah-MP (Nie et al., 2018).

However, most of these model development studies have focused on data-rich regions such as the US aquifer systems where groundwater is depleting alarmingly due to rapidly increased pumping for irrigation (Maxwell et al., 2015; Nie et al., 2019, 2021, 2022; Pokhrel et al., 2015), leaving major gaps that come with challenges, toward using the models in regions where groundwater issues are rapidly emerging, but data are scarce (Jayakumar and Lee, 2017). The MRB is a perfect example of such regions where upstream water management (Dang et al., 2016; Galelli et al., 2022; Hecht et al., 2019; Pokhrel et al., 2018a), climate change and variability (Arias et al., 2012; Delgado et al., 2012; Thompson et al., 2013), and increased groundwater pumping for domestic and irrigation uses are rapidly transforming groundwater dynamics but basin-scale groundwater modeling studies are rare, if not non-existent (Dang et al., 2016; Johnston and Kummu, 2012; Pokhrel et al., 2018a) primarily because of the basin wide data limitations to constrain and validate the model (Erban et al., 2014; Erban and Gorelick, 2016). Very crucially, leaving the growing anthropogenic influence aside, even the

natural dynamics of groundwater systems, especially over the entire MRB, is not adequately studied (Lacombe et al., 2017).

Further, growing number of observational studies have reported dramatic shifts in groundwater systems over the lower MRB (LMRB)especially the Mekong Delta region—due to the influence of growing anthropogenic activates over the past decade (Duy et al., 2021; Haddeland et al., 2006; Kazama et al., 2007; Lee et al., 2017; Loc et al., 2021; Tatsumi and Yamashiki, 2015; Tu et al., 2022a). Few studies investigated the historical groundwater situation at the sub-catchment level of the MRB under the influence of climate change, irrigation, and groundwater extraction (Gunnink et al., 2021; Hoanh et al., 2012; Shrestha et al., 2016; Tatsumi and Yamashiki, 2015). Other studies underlined the critical issues, such as groundwater pollution, and saltwater intrusion in the Mekong Delta and contaminant transport, that is directly linked with groundwater flow and groundwater depletion (Minderhoud et al., 2017; Tran et al., 2022). However, no basin scale groundwater study exists and process-based models have been rarely used to simulate these changes, resolve the interactions among various governing processes, and identify the key drivers (Johnston and Kummu, 2012). Fundamentally, little advancement has been made in understanding the critical controls of climate, physiography, and anthropogenic drivers on the dynamics of groundwater over the MRB.

Such lack of basin-scale groundwater modeling considering climatic and anthropogenic drivers critically hinders the understanding of evolving groundwater systems over the MRB, with implications on reliable future projections of water resource availability and use under climate change and intensified anthropogenic activities (Jasechko et al., 2014). Some global modeling studies have examined water and energy balances over the MRB (e.g., Haddeland et al., 2006; Lacombe et al., 2017; Tatsumi & Yamashiki, 2015; Felfelani et al., 2017). However, they have applied global models at a relatively coarse spatial resolution (e.g., 50-100 km), not accounting for finer scale processes including lateral flow (e.g., Felfelani et al., 2021; Krakauer et al., 2014) that are crucial in governing groundwater dynamics in the MRB's landscapes with high climatic, topographic, and hydrogeologic gradients (Cooper, 2010; Hung et al., 2012; Pokhrel et al., 2018a). Lastly, while some sub-basin scale studies have provided insights on local-scale groundwater changes, basin-scale and long-term (e.g., decadal evolutions) changes and patterns of groundwater dynamics for the MRB are largely lacking.

Here, we address the gaps identified above by focusing on the following three scientific contributions, and to advance groundwater modeling over the MRB. First, we present a fully distributed and process based LSM for the MRB, which simulates key hydrological processes on a full physical basis, including improved parameterizations for inter-grid lateral groundwater flow and aquifer pumping. Second, we use the model for a mechanistic investigation of interactions among the processes governing surface water and groundwater flows, including groundwater recharge and discharge, considering basin scale climatic drivers and human activities, and encompassing relatively fine scale process heterogeneities. Third, despite dearth of data to fully constrain the model, we present first-order quantification of the effects of increased irrigation and groundwater pumping on groundwater flow processes and storage dynamics over the LMRB.

We are aware of the challenges, and more so of the pressing need to improve our ability to simulate groundwater dynamics at the basin scale over the MRB. The primary goal is to capture the basin-scale patterns of groundwater dynamics and quantify the human-induced changes in groundwater systems; the underlying objective is to provide a foundational framework for basin wide groundwater studies in the MRB considering key governing processes and their response to the major climatic and human factors. Such a framework is expected to advance the current state of groundwater modeling in the MRB and open avenues for further research, including model enhancements. We address the following scientific questions: 1) How do climatic drivers, physiographic conditions, and topographic characteristics govern groundwater processes—specifically recharge, discharge, and lateral flow—across the

MRB? 2) What role does groundwater dynamics across the MRB play in modulating surface water systems in the LMRB? 3) How are anthropogenic activities—specifically irrigation and groundwater pumping—impacting groundwater systems in the LMRB? The model we use is the Community Land Model version 5 (CLM5) with the latest updates on groundwater parameterizations (see section 2.2).

2. Study area and methods

2.1. Study area

The MRB is shared by six countries in Southeast Asia: China, Myanmar, Lao PDR, Thailand, Cambodia, and Vietnam (MRC, 2005). The upper MRB (UMRB) is characterized by a steep narrow valley, with its geometry determined primarily by Himalayan orogeny (Carling, 2009). The LMRB can be divided into four regions: i) the northern Highlands, characterized by high elevation and dense vegetation, ii) the Khorat Plateau that includes much of the lowlands and a relatively flat landscape, iii) the Tonle Sap basin and iv) the Mekong Delta with an alluvial floodplain (Lacombe et al., 2017). The northern Highlands include the north of Thailand and Laos and extend into Vietnam. The Khorat Plateau covers most of northeast Thailand with its northern and eastern margin in central Laos and has a consistent basin elevation. Farther downstream, Tonle Sap Lake (TSL) covers the southern portion of Laos and most of Cambodia.

The climate across the MRB is tropical monsoonal. Precipitation patterns are seasonal, with the majority of annual totals occurring during the wet season between May and October (Kabir et al., 2022); the highest rainfall of over 2500 mm/yr occurs in the Highlands of Laos and the lowest of less than 1000 mm/yr over the Khorat Plateau in northeast Thailand. MRB is characterized by dense forest coverage towards the north and crop areas in the LMRB and Mekong Delta towards the south (Fig. 1). Surface water has historically been the dominant water resource for irrigation. However, over the past two decades, household wells and large-scale, deeper pumping for municipal and industrial purposes including irrigation have risen substantially (Hoanh et al., 2014). Currently, there are over one million wells in the Mekong Delta (Gunnink et al., 2021; Hoanh et al., 2014; Loc et al., 2021; Minderhoud et al., 2017) and the interest in further expanding the use of groundwater for agriculture is increasing (Tran et al., 2022).

2.2. Model

We use CLM5, which is the land component of the Community Earth System Model version 2 (CESM2) that resolves various surface and subsurface hydrological processes (e.g., soil and plant hydrology, snow physics, river routing, crop modeling) coupled with energy and biogeochemical (carbon and nitrogen) cycles on a complete physical basis (Danabasoglu et al., 2020). Although CLM5 and similar LSMs were traditionally designed to simulate surface water and energy fluxes within the Earth system model (ESM) frameworks, major advances have been made in recent years to represent sub-surface hydrological processes (Haddeland et al., 2011; Pokhrel et al., 2016). For example, CLM5 simulates key subsurface processes, including infiltration, plant hydraulics, soil moisture dynamics, and groundwater, that drive groundwater recharge on a full physical basis (Clark et al., 2015; Kennedy et al., 2019; Lawrence et al., 2019). Highly detailed groundwater models require extensive data and are exceedingly challenging to implement in the MRB, whereas simplistic process representation in parsimonious or lumped models can lead to uncertainties when hydrological processes are highly nonlinear or dynamic (Paniconi and Putti, 2015). Thus, we use CLM5, striking a balance between data requirements and process representation, and opening an opportunity to overcome the data challenge. The standard CLM5 includes a subsurface hydrology scheme with only a vertical exchange of water (Lawrence et al., 2019; Swenson et al., 2019). We use an advanced model version that includes the

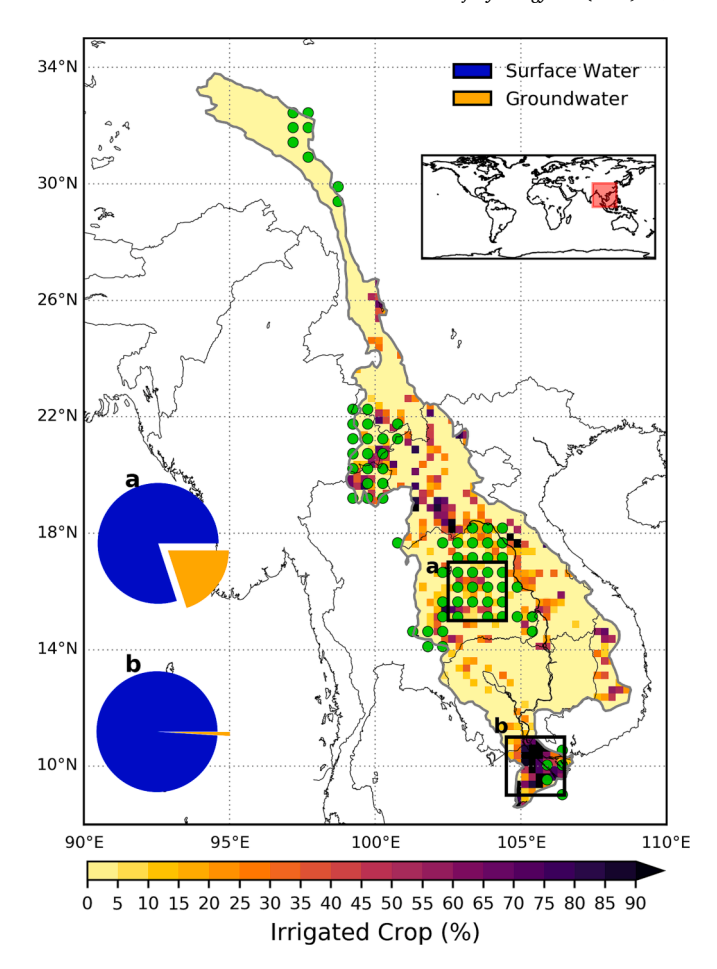


Fig. 1. Fractional area of irrigated cropland in the MRB with areas marked by green circles indicating groundwater-irrigated regions. The pie charts depict the groundwater use fraction for two selected regions marked with black squares where groundwater withdrawal for irrigation is relatively high. Upper right inset shows the location of the MRB in the global map. (For interpretation of the references to color in this figure legend, the reader is referred to the web version of this article.)

representation of lateral flow and aquifer pumping to account for the consumptive use of water for irrigation (Felfelani et al., 2021). The lateral groundwater flow is represented by Darcy's law following Fan et al. (2007), while the pumping scheme is based on HiGW-MAT model (Pokhrel et al., 2015).

The lateral flow is driven primarily by groundwater head difference-influenced by factors such as climate and topography (i.e., topographic slope in baseflow generation)—between two adjacent cells and computed based on Darcy's law (Fan and Li, 2013) as Qn = $WT(\frac{hn-hc}{l})$, where hn and hc are the hydraulic head in nth neighbor and center grid cells, respectively, T is the transmissivity, l is the distance between cells, and W = $\Delta x \sqrt{(0.5 \tan(\frac{\pi}{8}))}$ is the width of an imaginary octagon that replaces the square grid cell to provide an equal chance for all eight neighboring cells to interact with the center cell (Felfelani et al., 2021). When water table lies within the soil layer, the positive net lateral flow is added to soil layers in sequential order beginning from the soil layer right above the water table and the negative net lateral flow is removed from soil layers in sequential order beginning from the soil layer right below the water table (any residual is taken from the underlying aquifer layer) (Felfelani et al., 2021). When the water table is below the soil column, the net lateral flow is added (removed) to (from) the aquifer storage (Felfelani et al., 2021). Further details of the lateral flow and mass balance of each grid cell can be found in Felfelani et al., (2021). In CLM5 soil hydrologic processes are explicitly resolved up to

8.5 m depth and water table depth can vary from 0 to 80 m (Felfelani et al., 2021).

The subsurface is depicted using a high vertical resolution and improved solution to the Richard's equation to resolve soil water movement across layers (Felfelani et al., 2021). When unconfined aquifer under the soil column is activated, drainage from the lowest soil layer (recharge; q_{rech}) is controlled by a head-based lower boundary condition (i.e., $q_{rech}=q_i+\partial\theta_{liqi}rac{\partial q_i}{\partial\theta_{lioi}}$). Here, q_i is the water flux across the lowest interface and $heta q_{liqi}$ is the liquid volumetric soil moisture. When the water table is within the soil column, recharge rate is determined using Darcy's equation across the water table. In this configuration, subsurface runoff decays exponentially depending on the water table depth (z_{wt}), that is, $q_{sub} = \theta_{ice}q_{drai,max}$ exp ($-f_{drai}z_{wt}$), where, θ_{ice} is ice impedance factor, $q_{drai,max}$ is the maximum subsurface runoff when $z_{wt} =$ 0 and is set to $q_{drai,max} = 10 \sin(\beta)$; β is the mean grid cell topographic slope in radians and f_{drai} is the decay factor. f_{drai} is determined globally but can be calibrated to improve subsurface runoff simulations and streamflow at the regional scale.

2.2.1. Subsurface hydrologic parameters

Hydraulic properties of the soil are weighted combinations of the mineral properties, determined based on sand and clay contents (Clapp and Hornberger, 1978; Cosby et al., 1984) and organic properties of the soil (Lawrence and Slater, 2008). Hydraulic conductivity is defined at the depth of the interface between two adjacent soil layers and is a function of saturated hydraulic conductivity, the liquid volumetric soil moisture of the two layers and an ice impedance factor Θ_{ice} (NCAR, 2019). Note that the lateral hydraulic conductivity (K_{lat}) is determined from the vertical hydraulic conductivity (K_{ver})—resolved in the vertical one-dimensional soil movement—and percent of clay in the soil layer represents the anisotropy factor (i.e., $C_{clay} = K_{lat}/K_{ver}$) as described in Fan et al., (2007) and Zeng et al., (2016).

The prognostic aquifer transmissivity (T) is estimated based on the water table depth and hydraulic conductivity (Fan et al., 2007). If water table depth lies within the soil column, $T = T_1 + T_2$, where T_1 is the transmissivity of the saturated portion of the soil column (i.e., from the water table to the bottom most layer) and T_2 is the transmissivity of the depth below the bottom most layer (Felfelani et al., 2021). Here, T_2 is estimated using hydraulic conductivity of the bottom most layer, exponentially decayed with depth. A more in-depth discussion on the aquifer transmissivity estimation can be found in Felfelani et al., (2021) and Fan et al., (2007).

2.2.2. Irrigation parameterizations

Irrigation application is dynamically responsive to the simulated soil moisture conditions (Ozdogan et al., 2010). When irrigation is enabled, the crop areas of each grid cell are divided into irrigated and rainfed fractions based on a dataset of areas equipped for irrigation (Portmann et al., 2010). Irrigated and rainfed crops are placed on separate soil columns and irrigation is applied only to the irrigated portion. In irrigated croplands, a check is conducted once per day (in the first-time step after 6 AM local time) to determine whether irrigation is required on that day. Irrigation is triggered if crop leaf area index > 0, and the available soil moisture is below a specified threshold (Felfelani et al., 2018).

In the standard CLM5, irrigation water is applied to the soil column as an add-on to precipitation, withdrawing water from surface water (i. e., water in the main river channel) as a sole source of irrigation (NCAR, 2019). In the improved version of CLM5 used in this study, groundwater supplied fraction (provided in the model as input data) is extracted from the groundwater (from the aquifer or from the soil layers when water table is within soil column) and rest of the irrigation water requirement is withdrawn from the main channel (Felfelani et al., 2021). This model version is validated in continental US and found to adequately capture the subsurface dynamics as well as groundwater depletion (Felfelani

et al., 2021), adding confidence on the use of the model in other basin such as the MRB.

2.2.3. Surface water routing

To simulate streamflow, we use Model for Scale Adaptive River Transport (MOSART), a process-based model that uses kinematic wave formulations to route runoff as described in Li et al., (2015). The model uses a hydrography dataset, available globally at a spatial resolution of 0.125° . Topographic parameters such as flow direction, channel length, and channel slope, were obtained using the Dominant River Tracking (DRT) algorithm (Li et al., 2015); MOSART is the standard river routing scheme employed in CLM5.

2.3. Data

We use WATCH Forcing Data methodology applied to ERA-Interim reanalysis (WFDEI) global meteorological forcing data at 0.5° spatial resolution and 3-hour timely intervals (Weedon et al., 2014). WFDEI has been widely used in the LSM-based studies (Pinnington et al., 2018) and sensitivity analysis on the MRB by Kabir et al., (2022) suggests that WFDEI reproduce observed hydrological fluxes and states including streamflow, terrestrial water storage (TWS), and soil moisture in the MRB better than many other high-resolution climate forcing datasets. We utilize the International Geosphere-Biosphere Programme (IGBP) soil data to define soil characteristics at different soil layers.

We utilize the Global Map of Irrigated Areas version 5 (GMIAv5) (Siebert et al. 2015) for circa 2005, available at 0.083° spatial resolution (Figure S1) to specify the contribution of groundwater to total irrigation water withdrawals. In the MRB, fractional groundwater contribution varies substantially, ranging from 0 to 25% and with most groundwater irrigation areas found in northern Thailand (Figure S1). Irrigation is predominantly surface water based in other parts of the basin. The equilibrium water table depth (i.e., climatologic mean that represents the long-term balance between the climate-driven recharge and the topography-driven lateral flow) (Fan et al., 2013), aggregated to 0.05° resolution, is used to initialize the water table depth in CLM5 to reduce the spin-up period (Zeng et al., 2018). We use observed streamflow data from the Mekong River Commission (MRC) to validate streamflow simulations at six gauging locations across the basin.

To validate TWS, we use monthly Gravity Recovery and Climate Experiment (GRACE) data: two mass concentration (mascon) solutions from the Center for Space Research (CSR) (Save et al., 2016) at the University of Texas at Austin and Jet Propulsion Laboratory (JPL) (Watkins et al., 2014) at California Institute of Technology are used. To validate soil moisture, we use the data from Soil Moisture Active Passive (SMAP) satellite mission (Entekhabi et al., 2015); ground-based soil moisture data are not available for the MRB. There are no basin scale data available to reasonably validate simulated groundwater table. Thus, we used the synthesized data by digitizing the data published in the previous literature (Tiwari et al., 2023).

2.4. Experimental settings

We conduct four simulations with varied settings and time periods (Table 1) over the MRB at 0.05° spatial resolution (\sim 5 km). First, a multi-decadal simulation is performed without considering irrigation and pumping (i.e., natural state), referred to as the control (CTRL) simulation. This simulation is used to investigate the MRB's natural groundwater dynamics and its climatic and physiographic controls.

Then, we conduct three additional simulations with varying irrigation water use scenarios to investigate the role of irrigation and groundwater pumping in perturbing groundwater dynamics. The CTRL simulation is first spun up for 100 years by using WFDEI forcing data repeatedly for the year 1979. (Rodell et al., 2005). The CTRL simulation is performed without activating irrigation and pumping. The CTRL_SW is based on CTRL but activating irrigation where full irrigation demand

Table 1Experiments and Model Configurations.

Simulation	Irrigation	Pumping	Irrigation Water Source	Groundwater Use	Simulation Period
CTRL	No	No	No Irrigation	0	1979–2016
CTRL_SW	Yes	No	Surface Water	0	1979–2016
Sim_GWSW	Yes	Yes	Surface and	GMIAv5	2000-2016
			Groundwater		
Sim_GW	Yes	Yes	Groundwater	100 %	2000-2016

is met from surface water sources. Sim_GWSW is based on CTRL, with irrigation and groundwater pumping activated for conjunctive use from surface and groundwater. Sim_GW simulation represents a situation where the irrigation demand is met solely from groundwater. Since widespread irrigation in the MRB began in the 1990 s, we conduct Sim_GWSW and Sim_GW simulations for a shorter period beginning in 2000. Head-based lower boundary condition and lateral flow are active in all simulations. The experiments are designed to capture the natural groundwater dynamics of the MRB and the potential consequences of anthropogenic impacts such as irrigation and groundwater pumping.

3. Results

3.1. Surface and subsurface water variations

Comparison of the simulated monthly streamflow with observations

at six gauging stations across the LMRB indicates that the model performs well in capturing the temporal dynamics of streamflow and its seasonality (correlation coefficient ranges between 0.8 and 0.99 and NSE ranges between 0.7 and 0.95 across various stations). Given minimal precipitation during the dry season in the MRB (Hung et al., 2012; Pokhrel et al., 2018a; Sun et al., 2021), groundwater discharge is arguably the primary contributor to streamflow, particularly during this period. Thus, and given that no extensive basin-wide data exist for a direct groundwater validation, we focus on the evaluation of low flow indicators that serve as a proxy of groundwater discharge (i.e., baseflow) simulations (Yeh and Eltahir, 2005) along with a limited validation of simulated water table anomaly with observations. In general, flows having 85, 90, and 95 percent exceedance probability, i.e., Q85, Q90, and Q95, respectively, are simulated reasonably well across all stations (Fig. 2a-f). The mean percent deviation (MPD) of simulated and observed Q95, Q90, and Q85 ranges between 4 and 8%, 1.5-10%, and

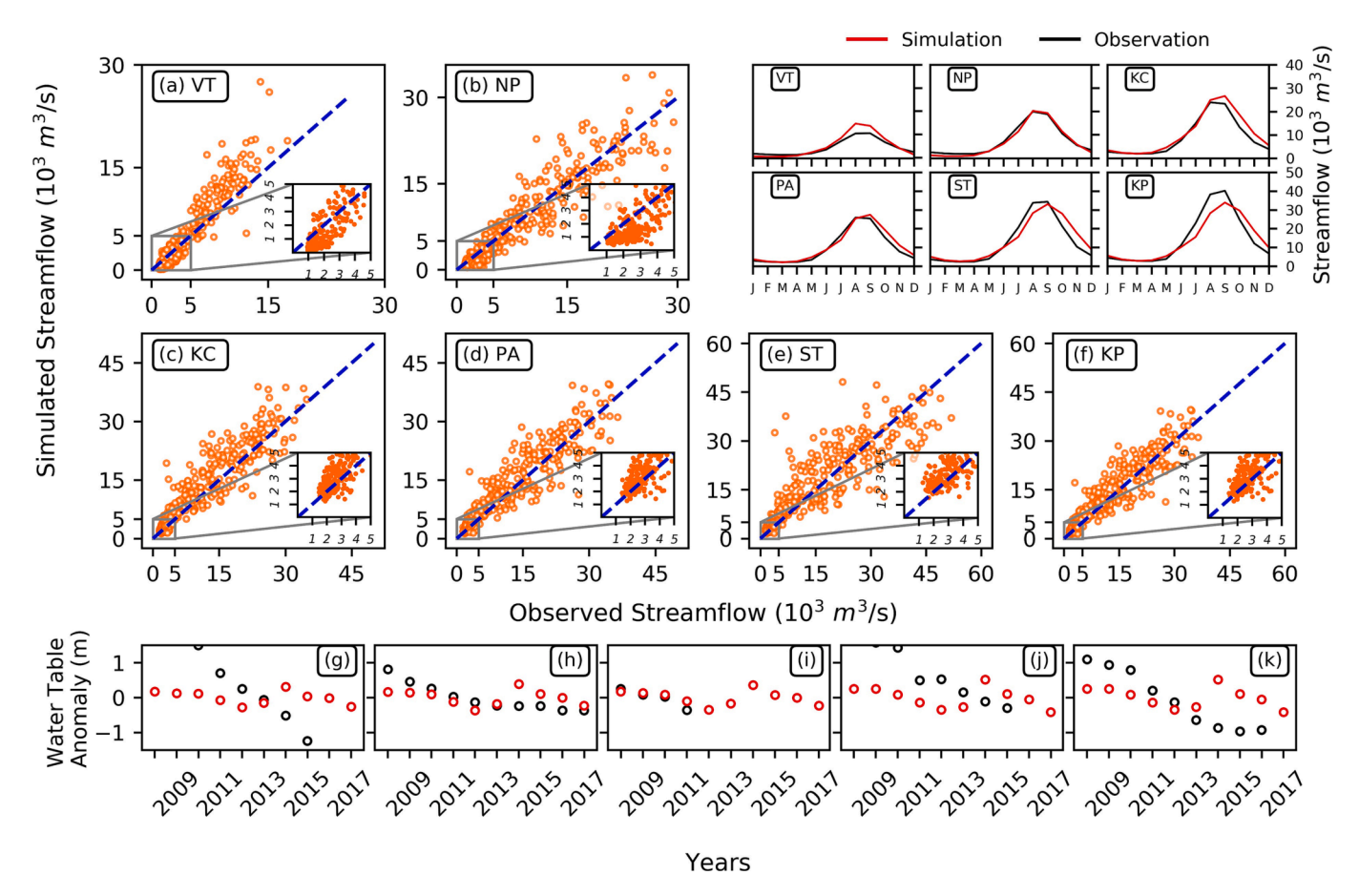


Fig. 2. Evaluation of simulated monthly streamflow (1979–2016) at six mainstream gauging stations in the LMRB: VT (Vientien), NP (Nakhon Phenom), KC (Kong Chiam), PA (Pakse), ST (Stung Treng), KP (Kampong Cham). The zoomed boxes in panels a-f depict the low flows for each station. The six subplots in the upper right panels represent a comparison of seasonal cycle of observed (black) and simulated (red) streamflow. The station locations are shown in Figure S2. Results presented here are based on Sim_GWSW simulation (see Table 1). Similar results, but on a daily scale, are presented in the supplementary material (Figure S3). Panels (g-k) show the comparison of the simulated water table anomaly with the observation (red: simulation; black: observation). Note that the mean of all available well heads within a given grid cell is used for a relatively consistent comparison of point data and grid-based simulations. Well locations are shown in the supplementary material (Figure S2). (For interpretation of the references to color in this figure legend, the reader is referred to the web version of this article.)

1.5–11%, respectively. These comparisons of annual and low flows as well as the temporal patterns suggest that the model reasonably simulates low flow, hence the underlying groundwater discharge or baseflow generation.

The temporal pattern of the simulated groundwater table anomaly represents a comparatively stable trend, unlike the observed water table changes in the MRB that depict a continuous decline from 2007 to 2016. This can be attributed to various factors including limitations in process representation, both natural and anthropogenic. Specifically, it is likely that the model does not capture the full range of groundwater dynamics driven by local scale processes that are reflected in the point measurements of groundwater table. Nevertheless, the model captures the declining trend of water table depletion, including some of the major

water table decline in 2010 and 2014 despite certain discrepancies in the magnitude (Fig. 2i-k). The model also captures some of the observed water table recoveries (Fig. 2k). The findings indicate that the model can reasonably capture the observed groundwater anomaly and inter-annual dynamics of groundwater changes. We note that a direct comparison between the water table derived from a 5 km model grid and very limited point-scale observations is not fully compatible; thus, these evaluations should be interpreted with sufficient caution. Further, there could be added uncertainties due to climate forcing particularly precipitation (Kabir et al., 2022), subsurface parameterization notably baseflow and insufficient representation of the groundwater irrigation areas that can lead to underestimation of water table decline. Most importantly, the validation locations are predominantly located in the

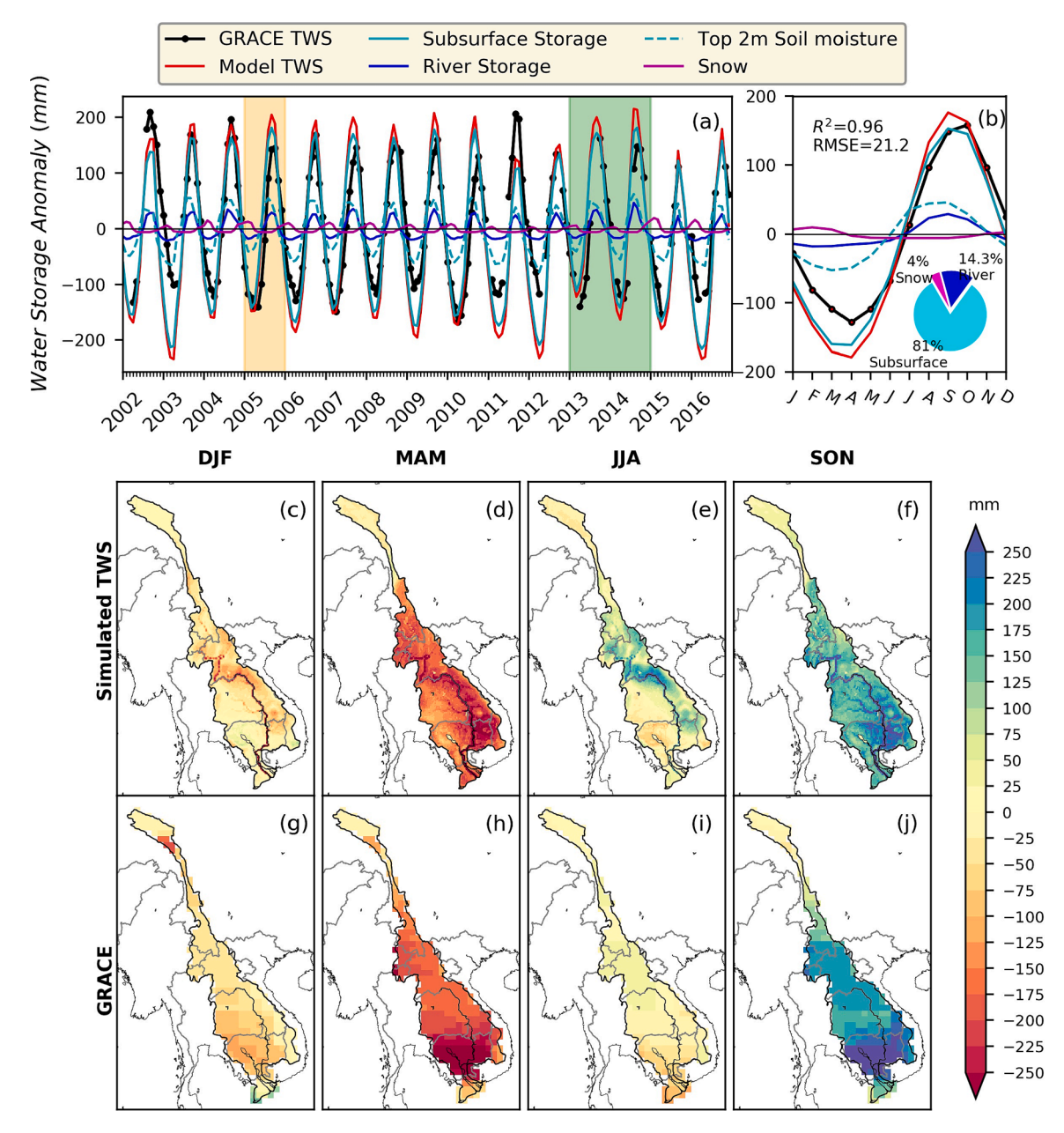


Fig. 3. Comparison of simulated and GRACE-based monthly terrestrial water storage anomaly averaged over the MRB for the 2002–2016 period (a). Simulated surface (river storage and snow) and subsurface water storage and its components (top 2 m soil moisture) are also shown. Individual components of surface water storage include water storage include water storage includes water storage i

Mekong Delta, where groundwater can be influenced by sea water intrusion and tides, factors currently not accounted for in the model. However, due to high data paucity (e.g., lack of basin-wide, continuous monitoring of groundwater levels), this is the only viable evaluation of our simulations in addition to the validation of discharge and TWS (Figs. 2 and 3). Given complex topographic features across the MRB, use of a global-scale LSM, and limited data to constrain process simulations, we consider these results to be satisfactory to study groundwater processes over the MRB.

Similar to streamflow, CLM5 well simulates the temporal variations of basin averaged TWS anomaly (Fig. 3). It is evident from Fig. 3 that the temporal variability is accurately reproduced along with the historical dry-wet transitions compared to GRACE observations (i.e., shaded areas in Fig. 3a). The good agreement with GRACE is evident not only visually but also statistically as indicated by a high R² (0.96) and low root mean square error (RMSE) (21.2 mm). However, the model did miss some of the events, such as in 2002 and 2011—two notable flood years in the MRB (Chinh et al., 2016; Dushmanta et al., 2007), and the simulated peak is slightly underestimated. Some of these underestimations and discrepancies are likely caused by limitations inherent in the model, such as absence of explicit representations of floodplain storage, particularly in the LMRB (Pokhrel et al., 2018). This limitation could have a noticeable impact on certain years, particularly those characterized by flood events.

We find that subsurface storage plays a critical role in modulating the total TWS variations and hence the hydrology of the MRB (Fig. 3a-b). Notably, subsurface storage accounts for ~ 81% of TWS amplitude, while groundwater anomaly explains 65% of the TWS anomaly in the MRB (subtracting soil moisture anomaly from the TWS anomaly). About 15% of the seasonal TWS amplitude is explained by surface water storage (Fig. 3b, pie chart), in line with the findings of previous studies (Pokhrel et al., 2018b) that reported this contribution to be ~13% based on a global LSM HiGW-MAT that is similar to CLM5 in process representation. Because GRACE provides the vertically integrated total TWS, not individual components, groundwater and surface water contribution could not be individually validated, and there are no other similar modeling studies for the entire MRB to cross-compare these individual TWS components. The comparison of seasonal TWS anomaly with GRACE data reveals that the overall seasonal variation is simulated reasonably well (Fig. 3c-j). Furthermore, the broad spatial pattern of the basin wide seasonal TWS anomaly is consistent with the GRACE data. However, some discrepancies are evident in the LMRB, likely due to uncertainty in precipitation (Kabir et al., 2022) in addition to model parameterizations. The ability to perform a more in-depth comparison with GRACE data is limited because of the inconsistency in spatial resolution between model and GRACE data.

We further compare simulated soil moisture with SMAP observations (Figure S4). Broad arid and humid contrasts of the soil moisture across

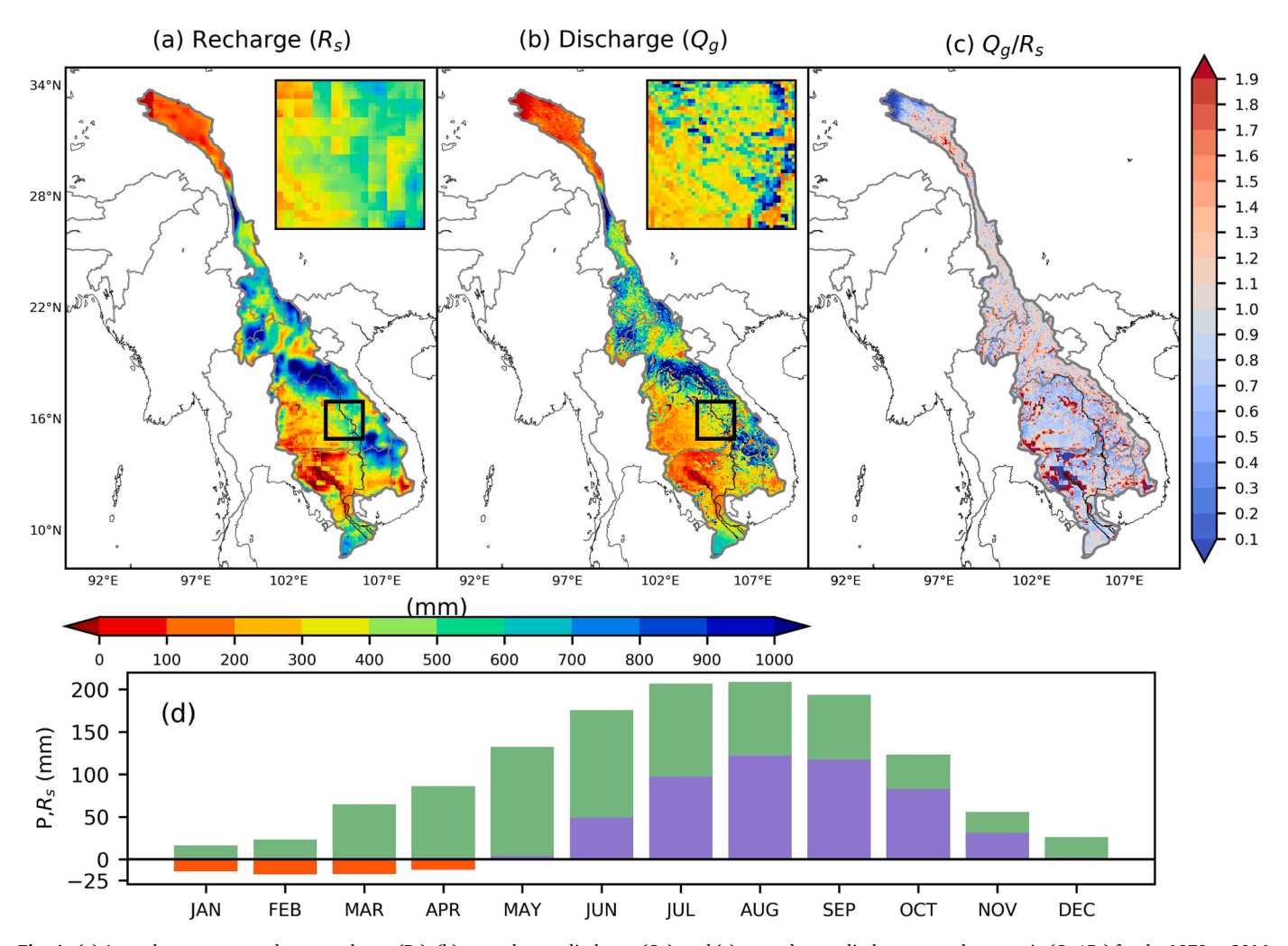


Fig. 4. (a) Annual average groundwater recharge (R_s) , (b) groundwater discharge (Q_g) , and (c) groundwater discharge to recharge ratio (Q_g/R_s) for the 1979 to 2016 period. Q_g/R_s less than 1 indicates groundwater contributor areas shown by different shades of blue, whereas $Q_g/R_s > 1$ marks groundwater receiver parts of the basin in different shades of red. The bottom panel (d) shows recharge (R_s) and precipitation (P) climatology for the same period. The results presented here are based on CTRL simulation. (For interpretation of the references to color in this figure legend, the reader is referred to the web version of this article.)

the basin are reasonably reproduced in the simulation. There are, however, some disagreements in the wet season (September-November), likely due to precipitation uncertainty (Kabir et al., 2022) or uncertainties in SMAP data (e.g., vegetation cover affects SMAP signal) (Colliander et al., 2020; Ma et al., 2017). These evaluations of TWS and soil moisture indicate that CLM5 simulates the subsurface hydrodynamics of the MRB reasonably well and could be used to examine the mechanistic interactions of the groundwater processes. Additionally, dominance of subsurface storage variation on TWS anomaly indicates a strong control of groundwater in MRB's water cycle and hence highlight the importance of improving groundwater processes understanding.

3.2. Groundwater flow patterns and drivers

Simulated annual average groundwater recharge in the MRB has distinct spatial variability, ranging from less than 100 mm/yr to over 1,000 mm/yr, with recharge rates generally decreasing from the UMRB to the LMRB (Fig. 4a). High recharge rates are simulated in regions (deep blue color in Fig. 4a) where precipitation rates are generally high. Laos and Vietnam are two such regions with high groundwater recharge and discharge rates. Some regions in the LMRB's floodplains are evident with net negative groundwater recharge (capillary rise) likely under shallow groundwater conditions, i.e., groundwater responds to soil moisture stress and contributes to evapotranspiration (ET). As expected, groundwater discharge follows similar spatial patterns of recharge (Fig. 4b). However, some areas with high recharge and low discharge rates are simulated (zoomed boxes in Fig. 4a and 4b), suggesting that

small-scale variations in soil characteristics and topographical factors govern regional groundwater flow and redistribute recharge spatially.

To provide further insights on relatively smaller scale processes and responses, we examine the basin-wide recharge to precipitation (R_s/P) ratio (Fig. 5a) and surface and subsurface fluxes in different regions across the MRB (Fig. 5b-m) that represent diverse topography, climate, soil, and vegetation characteristics. High precipitation during the wet season (June - September) is observed in locations b, c, and e. Similarly, high recharge and groundwater discharge are evident in these regions, with similar magnitude and climatological patterns. These regions in the UMRB are dominated by dense natural vegetation (Figure S5) and sandy soil deposits (~60 % sand content) (Figure S6) that favor precipitation infiltrating and generating high groundwater recharge (Fig. 5b-d). Thus, high R_s/P (i.e., R_s/P between 40 and 50%) is observed (Fig. 5b-d). In addition to soil and vegetation characteristics, the high climatic and topographic gradient affects groundwater flow that drives discharge to the surrounding valley regions. However, there is no linear correlation between groundwater recharge and discharge with the topographic slope. Other possible factors, such as low water table gradient and relatively homogeneous soil texture (dominated mainly by sandy soil deposits) (Figure S6), affect direct recharge and discharge impeding regional groundwater flow.

In contrast, relatively downstream towards the LMRB (Fig. 5f-g), R_s/P is rather high; however, relatively low discharge indicates possible control of local- to regional-scale groundwater flow. Topographic slope, soil characteristics, and water table gradient are likely to affect the divergence of groundwater discharge (Fig. 5f-g). Furthermore, more

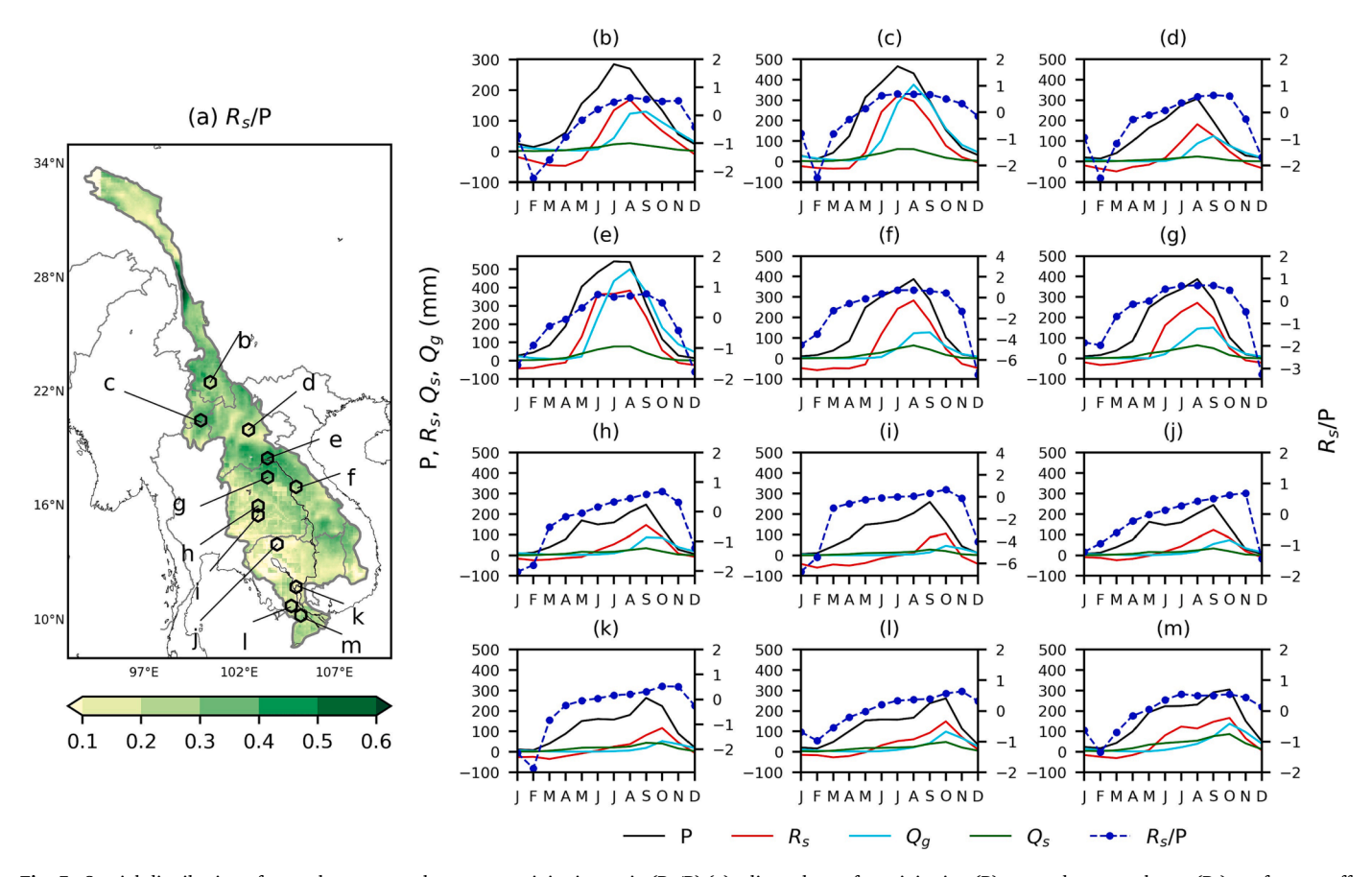


Fig. 5. Spatial distribution of annual average recharge to precipitation ratio (R_s/P) (a), climatology of precipitation (P), groundwater recharge (R_s), surface runoff (Q_s), groundwater discharge (Q_g) and R_s/P for different locations across the basin are shown in panels b-m. Locations are indicated in panel a (black hexagon). The results presented here are based on CTRL simulation for the 1979–2016 period. Locations b, c, and d exemplify topographically complex regions (high variations in topographic slope) in the northern mountainous areas with moderate to high precipitation. Locations e, f, and g illustrate a high permeability zone with intense precipitation. Conversely, locations h, i, and j have low permeability in the flat floodplains in the MRB around the TSL region. Lastly, locations k, l, and m represent the Mekong Delta.

heterogeneous soil composition is observed in these regions (Figure S6), which acts as the critical factor in controlling groundwater flow. For example, in the intermediate soil layers (Figure S6, layers 6–10), there is more heterogeneity in soil texture to impact groundwater flow paths. Relative control of regional flow owing to differences in topographic slope as well as heterogeneous soil characteristics is evident in the mountainous regions in the MRB (Fig. 5e-g).

Farther downstream in the LMRB floodplains (Fig. 5h-j), R_s/P is relatively low, in the order of \sim 10%, likely because the soil composition (alluvial clay is $\sim 60\%$ of the soil composition) inhibits quick percolation and recharge. Precipitation intensity is moderate in the LMRB floodplains. Also, in the wet season, relatively high soil moisture in the LMRB (Figure S4) can create soil saturation near the surface that virtually makes the soil impermeable and cause less recharge than in other regions (Fig. 5b-g). In addition, there is consistently high ET that leads to low groundwater recharge in comparison to the amount of water that infiltrates into the soil (Fig. 6). Therefore, despite the high or moderate precipitation rate, a relatively low recharge rate is evident. Thus, soil characteristics has a critical control over the groundwater flow in the LMRB floodplains. Besides, the low gradient in the water table influenced by flat topography in the LMRB floodplains controls the groundwater flow in this region, R_s/P varies in the Mekong Delta ranging from 0.2 to 0.4. Like the floodplain in the LMRB, high clay content in the soil inhibits groundwater recharge in the Mekong Delta. One primary reason for low recharge could be the presence of shallow clay layers (Figure S6), which act as a confining layer limiting recharge.

Similar findings in the Mekong Delta have also been reported by (Tu et al., 2022). Overall, climatic, and physiographic conditions, along with soil characteristics, play a crucial role in governing recharge and discharge. We note that we do not simulate the effects of dams and reservoirs that could influence groundwater recharge in the areas with substantial water impoundment.

The ratio of basin-wide discharge to recharge (Q_g/R_s) provides further insight into the groundwater flow pathways and the impacts of the basin-wide water budget. A vast majority of the basin area (indicated as different shades of blue color in Fig. 4c) is a groundwater receiver, suggesting that groundwater a dominant component of the basin-wide water budget in the LMRB. Overall, groundwater recharge and discharge zones follow the MRB's north-to-south and east-to-west topographic and climatic gradients.

3.3. Climatic control of groundwater flow

High recharge and discharge zones are generally located in areas with high annual precipitation and are strongly influenced by precipitation climatology. Basin averaged recharge rate peaks above 100 mm in August, the middle of the wet season in the MRB (Fig. 4d and Fig. 6). In contrast, recharge drops below 40 mm during the onset of the dry season in November. About 73% of annual recharge occurs between July and September, during which 40% of annual precipitation occurs (Fig. 4d and Figure S7). Precipitation and recharge in the basin are highly correlated ($\mathbb{R}^2=0.71$), suggesting a strong climate control on

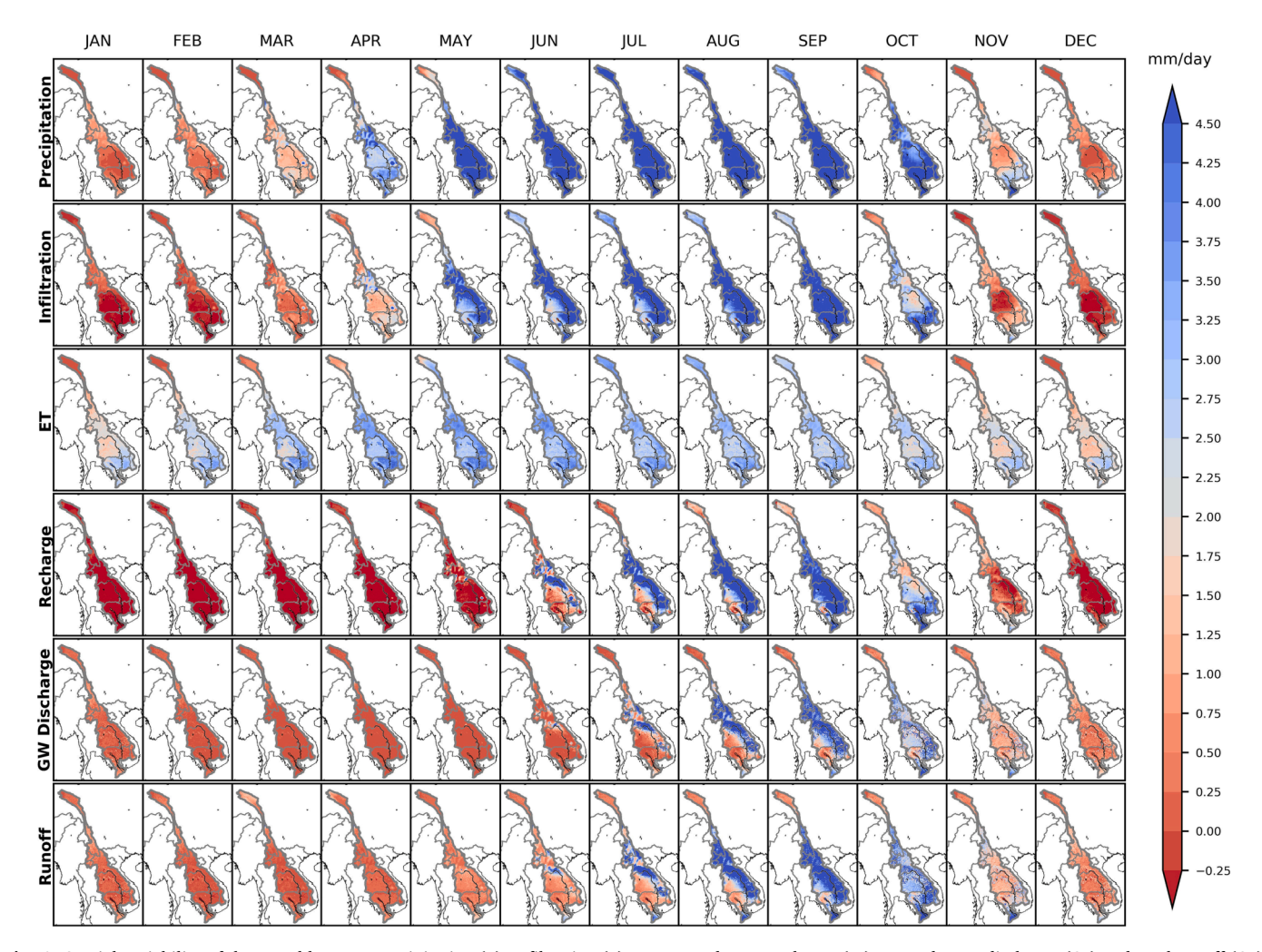


Fig. 6. Spatial variability of the monthly mean precipitation (P), Infiltration (I_f), ET, groundwater recharge (R_s), groundwater discharge (Q_g) and total runoff (Q_T) rates for the 1979–2016 period. The vertical panels represent different months.

groundwater variations. Across the basin, the average recharge-to-rainfall ratio is 34% annually and substantially higher during the wet season (\sim 52%) than during the dry season (\sim 6%), indicating that rainfall seasonality plays a crucial role in governing annual groundwater recharge. Therefore, wet-season rainfall substantially contributes to groundwater replenishment and can potentially buffer subsurface storage during drought. This is well studied and known in the Amazon River basin (Miguez-Macho and Fan, 2012a, 2012b; Pokhrel et al., 2013) but remains largely unexamined in the MRB.

3.4. Role of groundwater in surface water dynamics and governing drivers

Groundwater discharge over the MRB is simulated to be ~ 401 mm/yr, accounting for over 50% of annual river discharge (Fig. 5). Groundwater recharge and discharge peaks occur during the wet season with a 1–2 month delayed and dampened response to precipitation (Fig. 5b-h and Fig. 6). A shorter time lag between precipitation and infiltration is observed in the UMRB, which is characterized by sandy soil deposits that enhance rapid infiltration particularly during heavy rain events. Generally, we observe longer response time and high spatial variability toward the LMRB alluvial floodplains (Fig. 6). Groundwater

recharge and discharge have a 2-3 month delayed response to infiltration and precipitation in the LMRB, allowing groundwater recharge to carry over to the subsequent season and acts as a critical source of baseflow to rivers to maintain dry season flow. Also, comparable magnitude of basin-scale groundwater discharge and total runoff over the entire dry period (November-May) further underscores that groundwater supports the bulk of the total streamflow and its seasonal variation essentially governs surface water fluxes (Fig. 6). Further, a substantially higher negative R_s/P during the dry season (Fig. 5f and 5i) suggests that groundwater storage significantly contributes to augmenting soil moisture and ET. Particularly in the LMRB, some regions are evident where a negative R_s/P ratio is observed for consecutive 3-4 months after the offset of the wet season in September (Fig. 5e-g), suggesting that groundwater responds to soil moisture deficit for a considerable period when precipitation is low. Basin-wide negative recharge during December to May further indicates that groundwater acts as a basin-wide soil moisture buffer to support dry season soil moisture and ET (Fig. 6) implying that groundwater dynamics has a farreaching influence on the water and energy cycle in the MRB.

Overall, the interaction between groundwater and surface water in the MRB is regulated by a complex set of drivers, including seasonal

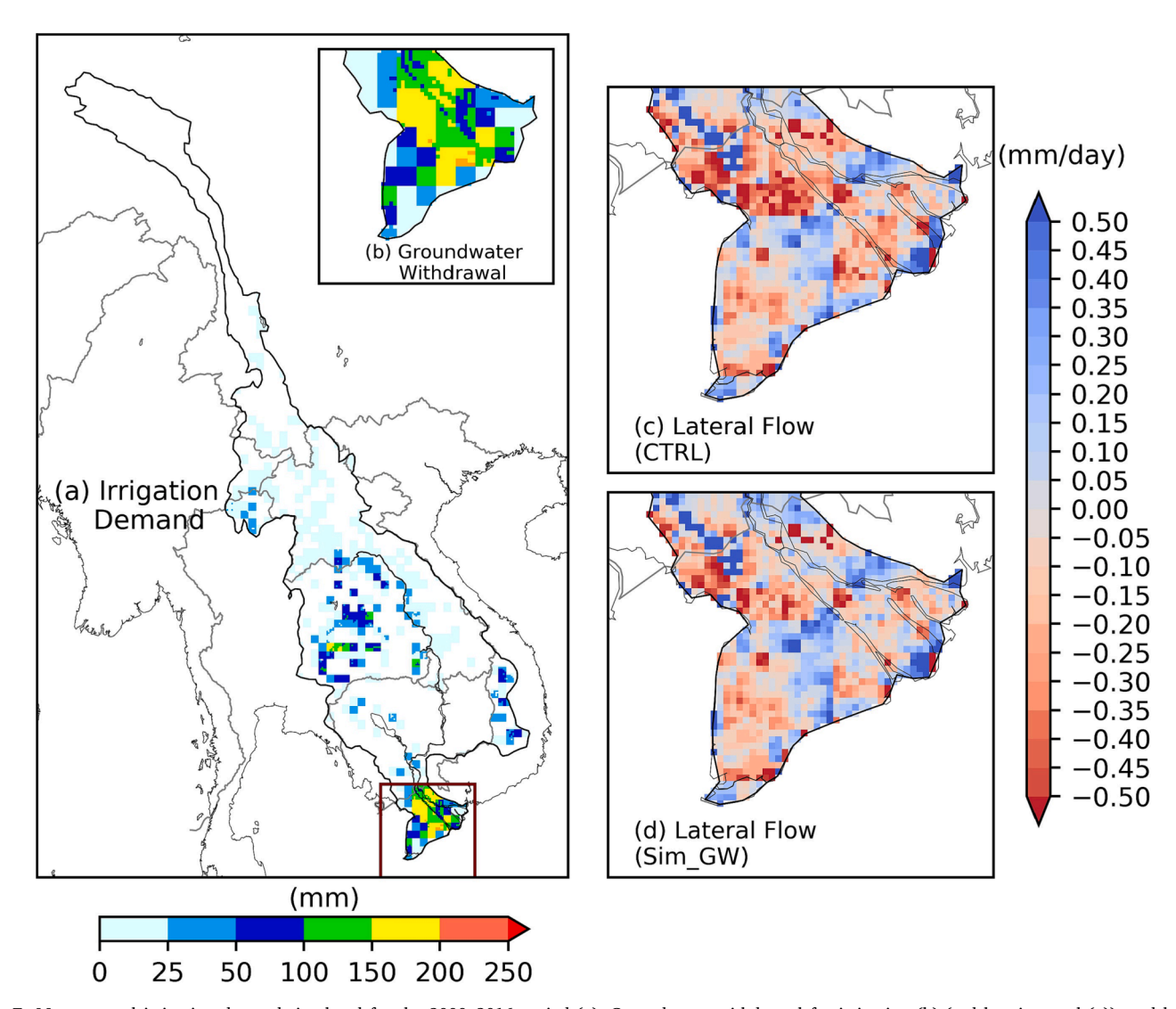


Fig. 7. Mean annual irrigation demand simulated for the 2000–2016 period (a). Groundwater withdrawal for irrigation (b) (red box in panel (a)), and lateral groundwater flow from CTRL (c) and Sim_GW (d) simulations over the Mekong Delta. Panel (c) and (d) share the same color bar. Units are indicated next to the color bars. Note that the groundwater supplied fraction of irrigation water demand is used around the year 2005 and made consistent throughout the simulation period of 2000–2016. (For interpretation of the references to color in this figure legend, the reader is referred to the web version of this article.)

variations in precipitation, soil properties and topography. The impacts of human activities, such as irrigation and groundwater pumping, are discussed in the later section. Notably, the results are simulation-based and depend on a variety of model parameterizations such as soil layer configurations, subsurface parameterizations, and input datasets used all of which are subject to certain degree of uncertainty, which all can affect simulation outcomes. However, our results provide detailed insights on the different groundwater processes from surface (infiltration) to the subsurface (groundwater discharge), leading to a mechanistic understanding on the dynamic interactions among the tightly coupled surface water-groundwater processes across the MRB.

3.5. Groundwater flow impacted by aquifer pumping

Finally, we examine how increased groundwater pumping for irrigation impacts groundwater systems in the MRB. We specifically quantify the changes in groundwater flow and water table depth caused by increased aquifer pumping for dry season irrigation. We focus on the Mekong Delta region that accounts for the majority of irrigated crops and where widespread irrigation is increasing in recent years; in other parts of the MRB, agricultural systems are mostly rainfed (Figure S8). The simulated annual irrigation demand in the MRB varies from ~ 25 to over 250 mm (Fig. 7a). In some portions of the Mekong Delta, irrigation demand is relatively high, for example, up to 200 mm/yr (Fig. 7a), and these results are consistent with previous estimates reported in global scale studies for year 2010 (Wada et al., 2016). Irrigation validation could be further enhanced by using satellite-based datasets (i.e., Brocca et al., (2018); Koch et al., (2020)). However, our results should be interpreted with caution because of possible uncertainties arising from the uncertainty in climate forcing and irrigation datasets used. Further, there could be under-representation of the recent irrigation development that is likely to cause an underestimated groundwater withdrawal.

A more in-depth evaluation is not possible because of the lack of spatially explicit datasets on irrigation withdrawals in the MRB.

Irrigation-pumping imposes a water table gradient, causing up to half a meter of water table decline in the Mekong Delta (Fig. 8a). In general, when averaged over a long period, the simulated effect of groundwater pumping is not substantial even in the Mekong Delta, especially in comparison to that in other major agricultural regions worldwide. This is so even when irrigation demand is met from the groundwater resource (i.e., Sim_GW simulation). Since irrigation development in the MRB is relatively recent (i.e., it started a few decades ago), long-term climate variability balances the pumping effects. However, widespread storage depletion is simulated in the Mekong Delta during the selected dry years (i.e., 2005 and 2015). The depletion is more than double in pumping cells in 2005 and 2015 compared to the long-term average water level decline and substantially large area of depletion is readily discernible (Fig. 8b-c). Depletion reaches ~ 1 m at the center of the Mekong Delta and ~ 0.5 m at the borders during 2005 under the increased influence of groundwater pumping (Sim GW simulation). These results are consistent with previous estimates reported by regional scale studies on the Mekong Delta, although the simulated absolute depletion may be underestimated because the information on the recent increase in groundwater pumping for irrigation (Minderhoud et al., 2020, 2017) is not accounted for in our model.

Water table gradient induces a shift in groundwater flow in the Mekong Delta (Fig. 8b-c), notably during dry years. The decline in water table (Fig. 8b) drives large flow towards the pumping cells from the surrounding, resulting in an increase in groundwater discharge in the neighboring cells (in Sim_GW simulation) (positive difference) compared to the CTRL simulation (Fig. 8e-f). Such pumping-induced alterations of groundwater dynamics, particularly during dry years, imply that groundwater depletion in the Mekong Delta could be exacerbated if prolonged droughts were to occur in the future.

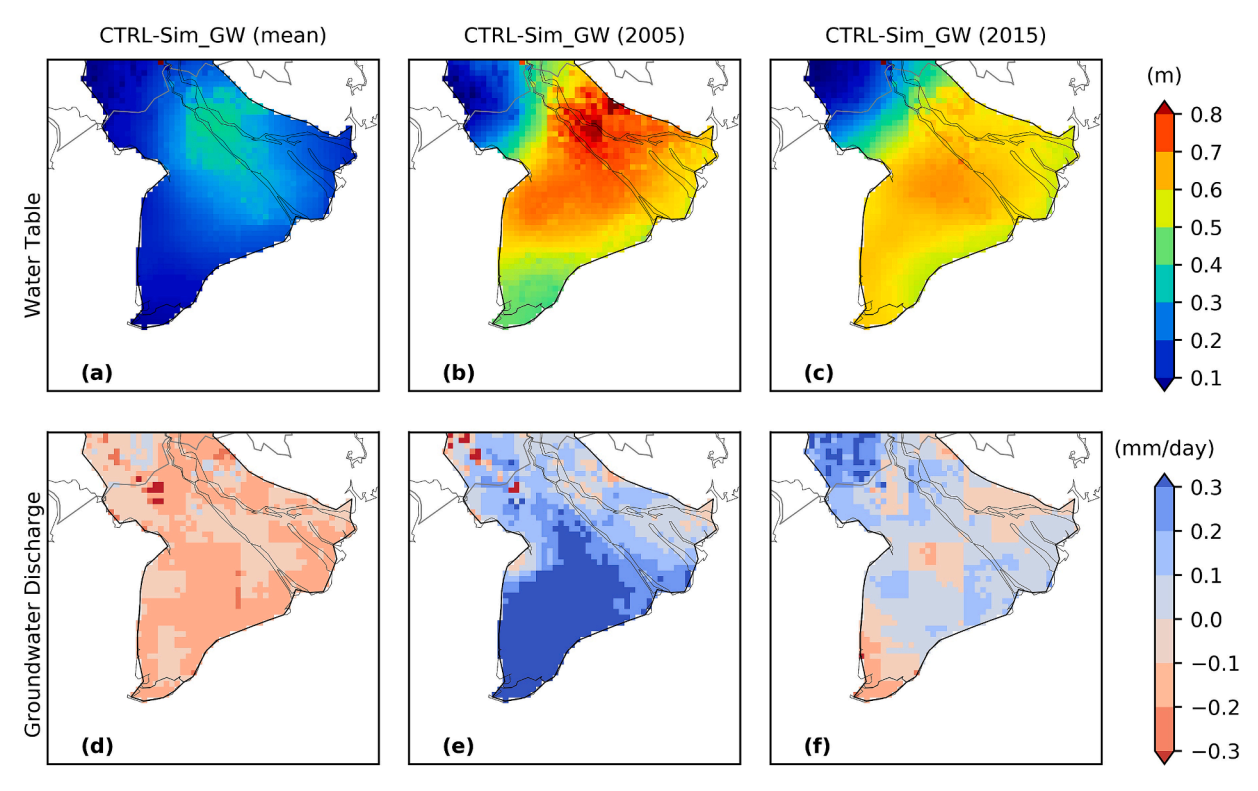


Fig. 8. Differences in water table depth and groundwater discharge between CTRL and Sim_GW simulations (see Table 1) for three different time windows (i.e., differences in long-term mean and two dry years of 2005 and 2015). Note that the mean represents the 2000–2016 period. Top row shows differences in water table depth (a, b and c) and bottom row shows differences in groundwater discharge (d, e and f). The color bars differ among top and bottom panels. Top color bar represents change in water table depth with larger positive values indicating a deeper water table (i.e., a decline) in Sim_GW simulation. Bottom color bar represents change in groundwater discharge (positive values indicate an increase in Sim_GW simulation).

The change in lateral groundwater flow (based on signs) further signifies the growing influence of irrigation and pumping on the region's groundwater systems (Fig. 7c-d). For instance, red cells in Fig. 7c (lateral outflow) turn blue (lateral inflow) due to the pumping-induced head gradient that triggers a substantial lateral flow towards the cone of depression (red blob, Fig. 8b). In general, groundwater withdrawals are likely to be unsustainable in the Mekong Delta if irrigation and pumping continue to expand in the future. Notably, the model shows promising potential to simulate irrigation and its influence on groundwater, and in identifying depletion hotspots. However, it is important to note that local scale phenomena such as cone of depression resulting from pumping-induced water table gradient may not have been captured adequately at the current spatial resolution (i.e., 5 km).

4. Conclusion

This study examines groundwater mechanisms, governing processes, and the interactions between groundwater and surface water under natural conditions and anthropogenic influences over the MRB using a fully distributed and process-based LSM with improved groundwater representation that accounts for lateral groundwater flow and aquifer pumping. Results are first validated with observed streamflow, water table, GRACE-based TWS, and SMAP-based soil moisture data, then used to examine groundwater flow processes across the MRB, the governing mechanism, and the effects of increasing irrigation activities on groundwater systems in the LMRB. The following summarizes the key findings of the study.

First, groundwater flow in the MRB exhibits high spatially heterogeneities, driven by a combination of factors including regional topography, climate, and local or regional scale subsurface characteristics. The climate (precipitation intensity and seasonality) has a first-order control on recharge and discharge variations across the basin. Further, regional subsurface characteristics dominantly control the recharge dynamics, especially in the LMRB. Second, in the LMRB, groundwater is the dominant source of streamflow, and its spatial variation and seasonality strongly modulate surface water dynamics; in some regions, groundwater perennially feeds streamflow. This mechanism is highlighted using an in-depth analysis over selected regions across the MRB with varying climatic, hydrologic, and geologic characteristics. Third, groundwater storage acts as a hydrological buffer and contributes substantially to soil moisture and ET for a considerable period of the year. These findings suggest a strong control of groundwater dynamics on the MRB's surface water and energy balances, with potential implications of perturbing the natural groundwater dynamics on surface water and energy fluxes. Fourth, groundwater use for irrigation has not had notable impact on groundwater dynamics over the long term, but the model simulates a region-wide storage depletion in the Mekong Delta during dry years, resulting in a shift in groundwater dynamics, also altering the magnitude and direction of groundwater discharge and lateral flow.

We note that our results are based on model simulations and may include uncertainties arising, for example, from forcing data, model resolution and imperfect groundwater parameterizations. Thus, the results should be interpreted with caution particularly for local scale implications of groundwater depletion hotspots and cone of depression. Further, the irrigation and groundwater data we used are from global databases, which may not include the most recent developments in groundwater irrigation, potentially underestimating the irrigationinduced changes in groundwater in the Mekong Delta. Our study offers a detailed discussion on the natural groundwater dynamics in the MRB as well as the potential impacts of irrigation development and groundwater withdrawal. A more comprehensive understanding of the groundwater dynamics in the MRB could require consideration of dams and reservoir operation in the simulation, which forms a potential avenue for future research. Future studies could address these limitations by further refining model parameterizations, particularly for subsurface runoff, improving process representation, and using any new datasets. Despite certain limitations, this study provides the first results on groundwater modeling for the entire MRB and by using a process-based LSM that includes a prognostic groundwater scheme and aquifer pumping for irrigation. Our study also advances groundwater modeling capabilities in data-limited regions such as the MRB.

CRediT authorship contribution statement

Tamanna Kabir: Conceptualization, Methodology, Formal analysis, Investigation, Data curation, Writing – original draft, Visualization. **Yadu Pokhrel:** Conceptualization, Methodology, Investigation, Resources, Writing – original draft, Supervision, Project administration, Funding acquisition. **Farshid Felfelani:** Writing – review & editing.

Declaration of Competing Interest

The authors declare that they have no known competing financial interests or personal relationships that could have appeared to influence the work reported in this paper.

Data availability

Data used in this study are available at https://doi.org/10.5281/zenodo.7968319 and https://doi.org/10.6084/m9.figshare.23154878.

Acknowledgements

This study was supported by the National Science Foundation (CAREER; Award# 1752729) and Belmont Forum Collaborative Research (BLUEGM; Award# 2127643). Simulations were conducted using computing resources from Cheyenne DOI (https://doi.org/10.5065/D6RX99HX): provided by NCAR's Computational and Information Systems Laboratory, sponsored by the NSF.

Appendix A. Supplementary data

Supplementary data to this article can be found online at https://doi.org/10.1016/j.jhydrol.2023.129761.

References

- Ambika, A.K., Mishra, V., 2019. Substantial decline in atmospheric aridity due to irrigation in India. Environ. Res. Lett. 15 https://doi.org/10.1088/1748-9326/ abs/8bc
- Arias, M.E., Cochrane, T.A., Piman, T., Kummu, M., Caruso, B.S., Killeen, T.J., 2012. Quantifying changes in flooding and habitats in the Tonle Sap Lake (Cambodia) caused by water infrastructure development and climate change in the Mekong Basin. J. Environ. Manage. 112, 53–66. https://doi.org/10.1016/j.ienyman.2012.07.003.
- Barlage, M., Chen, F., Rasmussen, R., Zhang, Z., Miguez-Macho, G., 2021. The Importance of Scale-Dependent Groundwater Processes in Land-Atmosphere Interactions Over the Central United States. Geophys. Res. Lett. 48, 1–10. https://doi.org/10.1029/2020GL092171.
- Brocca, L., Tarpanelli, A., Filippucci, P., Dorigo, W., Zaussinger, F., Gruber, A., Fernández-Prieto, D., 2018. How much water is used for irrigation? A new approach exploiting coarse resolution satellite soil moisture products. Int. J. Appl. Earth Obs. Geoinf. 73, 752–766. https://doi.org/10.1016/j.jag.2018.08.023.
- Carling, P.A., 2009. The Geology of the Lower Mekong River, 1st ed, The Mekong: Biophysical Environment of an International River Basin. Elsevier Inc. https://doi. org/10.1016/B978-0-12-374026-7.00002-4.
- Chinh, D.T., Bubeck, P., Dung, N.V., Kreibich, H., 2016. The 2011 flood event in the Mekong Delta: preparedness, response, damage and recovery of private households and small businesses. Disasters 40, 753–778. https://doi.org/10.1111/disa.12171.
- Clapp, R.B.A., Hornberger, G.M., 1978. Empirical Equations for Some Soil Hydraulic Properties 14.
- Clark, M.P., Fan, Y., Lawrence, D.M., Adam, J.C., Bolster, D., Gochis, D.J., Hooper, R.P., Kumar, M., Leung, L.R., Mackay, D.S., Maxwell, R.M., 2015. Improving the representation of hydrologic processes in Earth SystemModels 5929–5956. https://doi.org/10.1002/2015WR017096.Received.
- Colliander, A., Cosh, M.H., Kelly, V.R., Kraatz, S., Bourgeau-Chavez, L., Siqueira, P., Roy, A., Konings, A.G., Holtzman, N., Misra, S., Entekhabi, D., O'Neill, P., Yueh, S.

- H., 2020. SMAP Detects Soil Moisture Under Temperate Forest Canopies. Geophys. Res. Lett. 47, 1–10. https://doi.org/10.1029/2020GL089697.
- Condon, L.E., Kollet, S., Bierkens, M.F.P., Fogg, G.E., Maxwell, R.M., Hill, M.C., Fransen, H.J.H., Verhoef, A., Van Loon, A.F., Sulis, M., Abesser, C., 2021. Global Groundwater Modeling and Monitoring: Opportunities and Challenges. Water Resour. Res. 57, 1–27. https://doi.org/10.1029/2020WR029500.
- Cooper, M., 2010. Advanced Bash-Scripting Guide An in-depth exploration of the art of shell scripting Table of Contents. Okt 2005 Abrufbar uber httpwww tldp orgLDPabsabsguide pdf Zugriff 1112 2005 2274, 2267–2274. https://doi.org/ 10.1002/hyp.
- Cosby, B.J., Hornberger, G.M., Clapp, R.B., Ginn, T.R., 1984. Exploration of the Relationships of Soil Moisture Characteristics to the Physical Properties of Soils 20, 682-690
- Crosbie, R.S., Scanlon, B.R., Mpelasoka, F.S., Reedy, R.C., Gates, J.B., Zhang, L., 2013.

 Potential climate change effects on groundwater recharge in the High Plains Aquifer,
 USA. Water Resour. Res. 49, 3936–3951. https://doi.org/10.1002/wrcr.20292.
- Cuthbert, M.O., Gleeson, T., Moosdorf, N., Befus, K.M., Schneider, A., Hartmann, J., Lehner, B., 2019. Global patterns and dynamics of climate-groundwater interactions. Nat. Clim. Chang. 9, 137–141. https://doi.org/10.1038/s41558-018-0386.4
- Danabasoglu, G., Lamarque, J.F., Bacmeister, J., Bailey, D.A., DuVivier, A.K., Edwards, J., Emmons, L.K., Fasullo, J., Garcia, R., Gettelman, A., Hannay, C., Holland, M.M., Large, W.G., Lauritzen, P.H., Lawrence, D.M., Lenaerts, J.T.M., Lindsay, K., Lipscomb, W.H., Mills, M.J., Neale, R., Oleson, K.W., Otto-Bliesner, B., Phillips, A.S., Sacks, W., Tilmes, S., van Kampenhout, L., Vertenstein, M., Bertini, A., Dennis, J., Deser, C., Fischer, C., Fox-Kemper, B., Kay, J.E., Kinnison, D., Kushner, P. J., Larson, V.E., Long, M.C., Mickelson, S., Moore, J.K., Nienhouse, E., Polvani, L., Rasch, P.J., Strand, W.G., 2020. The Community Earth System Model Version 2 (CESM2). J. Adv. Model. Earth Syst. 12, 1–35. https://doi.org/10.1029/2019MS001916.
- Dang, T.D., Cochrane, T.A., Arias, M.E., Van, P.D.T., de Vries, T.T., 2016. Hydrological alterations from water infrastructure development in the Mekong floodplains. Hydrol. Process. 30, 3824–3838. https://doi.org/10.1002/hyp.10894.
- de Graaf, I.E.M., Gleeson, T., (Rens) van Beek, L.P.H., Sutanudjaja, E.H., Bierkens, M.F. P., 2019. Environmental flow limits to global groundwater pumping. Nature 574, 90–94. https://doi.org/10.1038/s41586-019-1594-4.
- De Graaf, I.E.M., Stahl, K., 2022. A model comparison assessing the importance of lateral groundwater flows at the global scale. Environ. Res. Lett. 17 https://doi.org/ 10.1088/1748-9326/ac50d2.
- De Graaf, I.E.M., Sutanudjaja, E.H., Van Beek, L.P.H., Bierkens, M.F.P., 2015. A highresolution global-scale groundwater model. Hydrol. Earth Syst. Sci. 19, 823–837. https://doi.org/10.5194/hess-19-823-2015.
- Delgado, J.M., Merz, B., Apel, H., 2012. A climate-flood link for the lower Mekong River. Hydrol. Earth Syst. Sci. 16, 1533–1541. https://doi.org/10.5194/hess-16-1533-2012
- Döll, P., 2009. Vulnerability to the impact of climate change on renewable groundwater resources: A global-scale assessment. Environ. Res. Lett. 4 https://doi.org/10.1088/ 1748-9326/4/3/035006.
- Dushmanta, D., Jahangir, A., Kazuo, U., Masayoshi, H., Sadayuki, H., 2007. A two-dimensional hydrodynamic model for flood inundation simulation: a case study in the lower Mekong river basin. Hydrol. Process. 2274, 2267–2274. https://doi.org/10.1002/hyp.
- Duy, N.L., Nguyen, T.V.K., Nguyen, D.V., Tran, A.T., Nguyen, H.T., Heidbüchel, I., Merz, B., Apel, H., 2021. Groundwater dynamics in the Vietnamese Mekong Delta: Trends, memory effects, and response times. J. Hydrol. Reg. Stud. 33, 100746 https://doi.org/10.1016/j.ejrh.2020.100746.
- E Condon, L., Maxwell, R.M., 2015. Evaluating the relationship between topography and groundwater using outputs from a continental-scale integrated hydrology model Laura. J. Am. Water Resour. Assoc. 5, 2. https://doi.org/10.1002/2014WR016774.
- Engdahl, N.B., 2017. Transient effects on confined groundwater age distributions: Considering the necessity of time-dependent simulations. Water Resour. Res. 53, 7332–7348. https://doi.org/10.1002/2016WR019916.
- Entekhabi, B.D., Njoku, E.G., Neill, P.E.O., Kellogg, K.H., Crow, W.T., Edelstein, W.N., Entin, J.K., Goodman, S.D., Jackson, T.J., Johnson, J., Kimball, J., Piepmeier, J.R., Koster, R.D., Martin, N., Mcdonald, K.C., Moghaddam, M., Moran, S., Reichle, R., Shi, J.C., Spencer, M.W., Thurman, S.W., Tsang, L., Zyl, J. Van, 2015. (SMAP) Mission 98.
- Erban, L.E., Gorelick, S.M., 2016. Closing the irrigation deficit in Cambodia: Implications for transboundary impacts on groundwater and Mekong River flow. J. Hydrol. 535, 85–92. https://doi.org/10.1016/j.jhydrol.2016.01.072.
- Erban, L.E., Gorelick, S.M., Zebker, H.A., 2014. Groundwater extraction, land subsidence, and sea-level rise in the Mekong Delta, Vietnam. Environ. Res. Lett. 9 https://doi.org/10.1088/1748-9326/9/8/084010.
- Evans, T.B., White, S.M., Wilson, A.M., 2020. Coastal Groundwater Flow at the Nearshore and Embayment Scales: A Field and Modeling Study. Water Resour. Res. 56, 1–15. https://doi.org/10.1029/2019WR026445.
- Fan, Y., Clark, M., Lawrence, D.M., Swenson, S., Band, L.E., Brantley, S.L., Brooks, P.D., Dietrich, W.E., Flores, A., Grant, G., Kirchner, J.W., Mackay, D.S., McDonnell, J.J., Milly, P.C.D., Sullivan, P.L., Tague, C., Ajami, H., Chaney, N., Hartmann, A., Hazenberg, P., McNamara, J., Pelletier, J., Perket, J., Rouholahnejad-Freund, E., Wagener, T., Zeng, X., Beighley, E., Buzan, J., Huang, M., Livneh, B., Mohanty, B.P., Nijssen, B., Safeeq, M., Shen, C., van Verseveld, W., Volk, J., Yamazaki, D., 2019. Hillslope Hydrology in Global Change Research and Earth System Modeling. Water Resour. Res. 1737–1772 https://doi.org/10.1029/2018WR023903.
- Fan, Y., Li, H., 2013. Global Patterns of Groundwater. Science. 339 (6122), 940–944. htt ps://www.science.org/doi/10.1126/science.1229881.

- Fan, Y., Miguez-Macho, G., Weaver, C.P., Walko, R., Robock, A., 2007. Incorporating water table dynamics in climate modeling: 1. Water table observations and equilibrium water table simulations. J. Geophys. Res. Atmos. 112, 1–17. https://doi. org/10.1029/2006JD008111.
- Fan, Y., Schaller, M.F., 2009. River basins as groundwater exporters and importers: Implications for water cycle and climate modeling. J. Geophys. Res. Atmos. 114 https://doi.org/10.1029/2008JD010636.
- Felfelani, F., Wada, Y., Longuevergne, L., Pokhrel, Y.N., 2017. Natural and humaninduced terrestrial water storage change: A global analysis using hydrological models and GRACE. J. Hydrol. 553, 105–118. https://doi.org/10.1016/j. ibydrol.2017.07.048.
- Felfelani, F., Pokhrel, Y., Guan, K., Lawrence, D.M., 2018. Utilizing SMAP Soil Moisture Data to Constrain Irrigation in the Community Land Model. Geophys. Res. Lett. 45, 12892–12902. https://doi.org/10.1029/2018GL080870.
- Felfelani, F., Lawrence, D.M., Pokhrel, Y., 2021. Representing Intercell Lateral Groundwater Flow and Aquifer Pumping in the Community Land Model. Water Resour. Res. 57, 1–24. https://doi.org/10.1029/2020WR027531.
- Fenicia, F., Savenije, H.H.G., Margen, P., Pfister, L., 2006. Is the groundwater reservoir linear? Learning from data in hydrological modelling. Hydrol. Earth Syst. Sci. 10, 139–150. https://doi.org/10.5194/hess-10-139-2006.
- Fenicia, F., Kavetski, D., Savenije, H.H.G., 2011. Elements of a flexible approach for conceptual hydrological modeling: 1. Motivation and theoretical development 47, 1–13. https://doi.org/10.1029/2010WR010174.
- Ferguson, I.M., Maxwell, R.M., 2010. Role of groundwater in watershed response and land surface feedbacks under climate change. Water Resour. Res. 46, 1–15. https:// doi.org/10.1029/2009WR008616.
- Galelli, S., Dang, T.D., Ng, J.Y., Chowdhury, A.F.M.K., Arias, M.E., 2022. Opportunities to curb hydrological alterations via dam re-operation in the Mekong. Nat. Sustain. https://doi.org/10.1038/s41893-022-00971-z.
- Gleeson, T., Wada, Y., Bierkens, M.F.P., Van Beek, L.P.H., 2012. Water balance of global aquifers revealed by groundwater footprint. Nature 488, 197–200. https://doi.org/ 10.1038/nature11295.
- Gleeson, T., Befus, K.M., Jasechko, S., Luijendijk, E., Cardenas, M.B., 2016. The global volume and distribution of modern groundwater. Nat. Geosci. 9, 161–164. https:// doi.org/10.1038/ngeo2590.
- Gleeson, T., Wagener, T., Döll, P., Zipper, S.C., West, C., Wada, Y., Taylor, R., Scanlon, B., Rosolem, R., Rahman, S., Oshinlaja, N., Maxwell, R., Lo, M.H., Kim, H., Hill, M., Hartmann, A., Fogg, G., Famiglietti, J.S., Ducharne, A., De Graaf, I., Cuthbert, M., Condon, L., Bresciani, E., Bierkens, M.F.P., 2021. GMD perspective: The quest to improve the evaluation of groundwater representation in continental-to global-scale models. Geosci. Model Dev. 14, 7545–7571. https://doi.org/10.5194/gmd-14-7545-2021.
- Gleick, P.H., 2018. The World's. Water Volume 9. The report on freshwater resources. Gunnink, J., Pham, H.V., Oude Essink, G., Bierkens, M., 2021. The 3D groundwater salinity distribution and fresh groundwater volumes in the Mekong Delta, Vietnam, inferred from geostatistical analyses. Earth Syst. Sci. Data Discuss. 4441776, 1–31. https://doi.org/10.5194/essd-2021-15.
- Haddeland, I., Clark, D.B., Franssen, W., Ludwig, F., Voß, F., Arnell, N.W., Bertrand, N., Best, M., Folwell, S., Gerten, D., Gomes, S., Gosling, S.N., Hagemann, S., Hanasaki, N., Harding, R., Heinke, J., Kabat, P., Koirala, S., Oki, T., Polcher, J., Stacke, T., Viterbo, P., Weedon, G.P., and Pat Yeh, 2011. Multimodel Estimate of the Global Terrestrial Water Balance: Setup and First Results 869–884. https://doi.org/10.1175/2011JHM1324.1.
- Haddeland, I., Lettenmaier, D.P., Skaugen, T., 2006. Effects of irrigation on the water and energy balances of the Colorado and Mekong river basins. J. Hydrol. 324, 210–223. https://doi.org/10.1016/j.jhydrol.2005.09.028.
- Hanasaki, N., Fujimori, S., Yamamoto, T., Yoshikawa, S., Masaki, Y., Hijioka, Y., Kainuma, M., Kanamori, Y., Masui, T., Takahashi, K., Kanae, S., 2013. A global water scarcity assessment under Shared Socio-economic Pathways Part 1: Water use. Hydrol. Earth Syst. Sci. 17, 2375–2391. https://doi.org/10.5194/hess-17-2375-2013.
- Hecht, J.S., Lacombe, G., Arias, M.E., Dang, T.D., Piman, T., 2019. Hydropower dams of the Mekong River basin: A review of their hydrological impacts. J. Hydrol. 568, 285–300. https://doi.org/10.1016/j.jhydrol.2018.10.045.
- Hoang, L.P., van Vliet, M.T.H., Kummu, M., Lauri, H., Koponen, J., Supit, I., Leemans, R., Kabat, P., Ludwig, F., 2019. The Mekong's future flows under multiple drivers: How climate change, hydropower developments and irrigation expansions drive hydrological changes. Sci. Total Environ. 649, 601–609. https://doi.org/10.1016/j.scitotenv.2018.08.160.
- Hoanh, C.T., Facon, T., Thuon, T., Bastakoti, R.C., Molle, F., Phengphaengsy, F., 2012. Irrigation in the lower mekong basin countries: The beginning of a new era? Contested Waterscapes Mekong Reg. Hydropower, Livelihoods Gov. 9781849770, 143–172. https://doi.org/10.4324/9781849770866.
- Hoanh, C.T., Suhardiman, D., Anh, L.T., 2014. Irrigation development in the Vietnamese Mekong Delta: Towards polycentric water governance? Int. J. Water Gov. 2, 61–82. https://doi.org/10.7564/14-ijwg59.
- Hung, N.N., Delgado, J.M., Tri, V.K., Hung, L.M., Merz, B., Bárdossy, A., Apel, H., 2012. Floodplain hydrology of the mekong delta. Vietnam. Hydrol. Process. 26, 674–686. https://doi.org/10.1002/hyp.8183.
- Jasechko, S., Jean, B.S., Gleeson, T., Wada, Y., Fawcett, P.J., Sharp, 1, Z.D., J., M.J., Welker, J.M., 2014. The pronounced seasonality of global groundwater recharge 5375–5377. https://doi.org/10.1002/2013WR014979.Reply.
- Jayakumar, R., Lee, E., 2017. Climate change and groundwater conditions in the Mekong Region-A review. J. Groundw. Sci. Eng. 5, 14–30.
- Johnston, R., Kummu, M., 2012. Water Resource Models in the Mekong Basin: A Review. Water Resour. Manag. 26, 429–455. https://doi.org/10.1007/s11269-011-9925-8.

- Kabir, T., Pokhrel, Y., Felfelani, F., 2022. On the Precipitation-Induced Uncertainties in Process-Based Hydrological Modeling in the Mekong River Basin. Water Resour. Res. 58. https://doi.org/10.1029/2021WR030828.
- Kazama, S., Hagiwara, T., Ranjan, P., Sawamoto, M., 2007. Evaluation of groundwater resources in wide inundation areas of the Mekong River basin. J. Hydrol. 340, 233–243. https://doi.org/10.1016/j.jhydrol.2007.04.017.
- Kennedy, D., Swenson, S., Oleson, K.W., Lawrence, D.M., Fisher, R., Carlos, A., Gentine, P., 2019. Implementing Plant Hydraulics in the Community Land Model, Version 5 Journal of Advances in Modeling Earth Systems. https://doi.org/10.1029/2018MS001500.
- Kluzek, E., 2013. CESM Research Tools: CLM4 in Documentation.
- Koch, J., Zhang, W., Martinsen, G., He, X., Stisen, S., 2020. Estimating Net Irrigation Across the North China Plain Through Dual Modeling of Evapotranspiration. Water Resour. Res. 56 https://doi.org/10.1029/2020WR027413.
- Koirala, S., Yeh, P.J.F., Hirabayashi, Y., Kanae, S., Oki, T., 2014. Global-scale land surface hydrologic modeling with the representation of water table dynamics. J. Geophys. Res. 119, 75–89. https://doi.org/10.1002/2013JD020398.
- Koirala, S., Kim, H., Hirabayashi, Y., Kanae, S., Oki, T., 2019. Sensitivity of Global Hydrological Simulations to Groundwater Capillary Flux Parameterizations. Water Resour. Res. 55, 402–425. https://doi.org/10.1029/2018WR023434.
- Kollet, S.J., Maxwell, R.M., 2008. Capturing the influence of groundwater dynamics on land surface processes using an integrated, distributed watershed model. Water Resour. Res. 44, 1–18. https://doi.org/10.1029/2007WR006004.
- Krakauer, N.Y., Li, H., Fan, Y., 2014. Groundwater flow across spatial scales: Importance for climate modeling. Environ. Res. Lett. 9 https://doi.org/10.1088/1748-9326/9/ 3/034003
- Kumar, P., Zhang, Y., Ma, N., Mishra, A., Panigrahy, N., 2021. Selecting hydrological models for developing countries: Perspective of global, continental, and country scale models over catchment scale models. J. Hydrol. 600, 126561 https://doi.org/ 10.1016/j.jhydrol.2021.126561.
- Lacombe, G., Douangsavanh, S., Vongphachanh, S., Pavelic, P., 2017. Regional assessment of groundwater recharge in the lower mekong basin. Hydrology 4, 1–18. https://doi.org/10.3390/hydrology4040060.
- Lawrence, D.M., Slater, Æ.A.G., 2008. Incorporating organic soil into a global climate model 145–160. https://doi.org/10.1007/s00382-007-0278-1.
- Lawrence, D.M., Fisher, R.A., Koven, C.D., Oleson, K.W., Swenson, S.C., Bonan, G., Collier, N., Ghimire, B., 2019a. The Community Land Model Version 5: Description of New Features. Benchmarking, and Impact of Forcing Uncertainty Journal of Advances in Modeling Earth Systems 5, 4245–4287. https://doi.org/10.1029/2018MS001583.
- Lawrence, D.M., Fisher, R.A., Koven, C.D., Oleson, K.W., Swenson, S.C., Bonan, G.,
 Collier, N., Ghimire, B., Kampenhout, L., Kennedy, D., Kluzek, E., Lawrence, P.J.,
 Li, F., Li, H., Lombardozzi, D., Riley, W.J., Sacks, W.J., Shi, M., Vertenstein, M.,
 Wieder, W.R., Xu, C., Ali, A.A., Badger, A.M., Bisht, G., Broeke, M., Brunke, M.A.,
 Burns, S.P., Buzan, J., Clark, M., Craig, A., Dahlin, K., Drewniak, B., Fisher, J.B.,
 Flanner, M., Fox, A.M., Gentine, P., Hoffman, F., Keppel-Aleks, G., Knox, R.,
 Kumar, S., Lenaerts, J., Leung, L.R., Lipscomb, W.H., Lu, Y., Pandey, A., Pelletier, J.
 D., Perket, J., Randerson, J.T., Ricciuto, D.M., Sanderson, B.M., Slater, A., Subin, Z.
 M., Tang, J., Thomas, R.Q., Val Martin, M., Zeng, X., 2019b. The Community Land
 Model Version 5: Description of New Features, Benchmarking, and Impact of Forcing
 Uncertainty. J. Adv. Model. Earth Syst. 11, 4245–4287. https://doi.org/10.1029/
 2018MS001583.
- Lee, E., Ha, K., Thi Minh Ngoc, N., Surinkum, A., Jayakumar, R., Kim, Y., Bin Hassan, K., 2017. Groundwater status and associated issues in the Mekong-Lancang River Basin: International collaborations to achieve sustainable groundwater resources. J. Groundw. Sci. Eng. 5, 1–13.
- Leng, G., Huang, M., Tang, Q., Gao, H., Leung, L.R., 2014. Modeling the effects of groundwater-fed irrigation on terrestrial hydrology over the conterminous United States. J. Hydrometeorol. 15, 957–972. https://doi.org/10.1175/JHM-D-13-049.1. Li, H.Y., Leung, L.R., Getirana, A., Huang, M., Wu, H., Xu, Y., Guo, J., Voisin, N., 2015.
- Li, H.Y., Leung, L.R., Getirana, A., Huang, M., Wu, H., Xu, Y., Guo, J., Voisin, N., 2015 Evaluating global streamflow simulations by a physically based routing model coupled with the community land model. J. Hydrometeorol. 16, 948–971. https:// doi.org/10.1175/JHM-D-14-0079.1.
- Liang, X., Xie, Z., Huang, M., 2003. A new parameterization for surface and groundwater interactions and its impact on water budgets with the variable infiltration capacity (VIC) land surface model. J. Geophys. Res. Atmos. 108 https://doi.org/10.1029/ 2002id003090
- Loc, H.H., Van Binh, D., Park, E., Shrestha, S., Dung, T.D., Son, V.H., Truc, N.H.T., Mai, N.P., Seijger, C., 2021. Intensifying saline water intrusion and drought in the Mekong Delta: From physical evidence to policy outlooks. Sci. Total Environ. 757, 143919 https://doi.org/10.1016/j.scitotenv.2020.143919.
- Ma, C., Li, X., Wei, L., Wang, W., 2017. Multi-scale validation of SMAP soil moisture products over cold and arid regions in Northwestern China using distributed ground observation data. Remote Sens. 9 https://doi.org/10.3390/rs9040327.
- Maxwell, R.M., Condon, L.E., Kollet, S.J., 2015. A high-resolution simulation of groundwater and surface water over most of the continental US with the integrated hydrologic model ParFlow v3. Geosci. Model Dev. 8, 923–937. https://doi.org/ 10.5194/gmd-8-923-2015.
- Maxwell, R.M., Kollet, S.J., 2008. Interdependence of groundwater dynamics and landenergy feedbacks under climate change. Nat. Geosci. 1, 665–669. https://doi.org/ 10.1038/ngeo315.
- Mcguire, K.J., Mcdonnell, J.J., 2010. Hydrological connectivity of hillslopes and streams: Characteristic time scales and nonlinearities 46, 1–17. https://doi.org/10.1029/2010WR009341.

- Megdal, S.B., Gerlak, A.K., Varady, R.G., Huang, L.Y., 2015. Groundwater Governance in the United States: Common Priorities and Challenges. Groundwater 53, 677–684. https://doi.org/10.1111/gwat.12294.
- Miguez-Macho, G., Fan, Y., 2012a. The role of groundwater in the Amazon water cycle: 1. Influence on seasonal streamflow, flooding and wetlands. J. Geophys. Res. Atmos. 117, 1–30. https://doi.org/10.1029/2012JD017539.
- Miguez-Macho, G., Fan, Y., 2012b. The role of groundwater in the Amazon water cycle:

 2. Influence on seasonal soil moisture and evapotranspiration. J. Geophys. Res.

 Atmos. 117 https://doi.org/10.1029/2012JD017540.
- Minderhoud, P.S.J., Erkens, G., Pham, V.H., Bui, V.T., Erban, L., Kooi, H., Stouthamer, E., 2017. Impacts of 25 years of groundwater extraction on subsidence in the Mekong delta. Vietnam. Environ. Res. Lett. 12 https://doi.org/10.1088/1748-9326/aa7146.
- Minderhoud, P.S.J., Middelkoop, H., Erkens, G., Stouthamer, E., 2020. Groundwater extraction may drown mega-delta: Projections of extraction-induced subsidence and elevation of the mekong delta for the 21st century. Environ. Res. Commun. 2 https:// doi.org/10.1088/2515-7620/ab5e21.
- MRC, 2005. Water used for agriculture in the Lower Mekong Basin 11, 1489–1683. NCAR, 2019. CLM5 Documentation Release 337.
- Nguyen, T.T.H., de Bie, C.A.J.M., Ali, A., Smaling, E.M.A., Chu, T.H., 2012. Mapping the irrigated rice cropping patterns of the Mekong delta, Vietnam, through hypertemporal spot NDVI image analysis. Int. J. Remote Sens. 33, 415–434. https://doi. org/10.1080/01431161.2010.532826.
- Nie, W., Zaitchik, B.F., Rodell, M., Kumar, S.V., Anderson, M.C., Hain, C., 2018. Groundwater Withdrawals Under Drought: Reconciling GRACE and Land Surface Models in the United States High Plains Aquifer. Water Resour. Res. 54, 5282–5299. https://doi.org/10.1029/2017WR022178.
- Nie, W., Zaitchik, B.F., Rodell, M., Kumar, S.V., Arsenault, K.R., Li, B., Getirana, A., 2019. Assimilating GRACE Into a Land Surface Model in the Presence of an Irrigation-Induced Groundwater Trend. Water Resour. Res. 55, 11274–11294. https://doi.org/10.1029/2019WR025363.
- Nie, W., Zaitchik, B.F., Rodell, M., Kumar, S.V., Arsenault, K.R., Badr, H.S., 2021. Irrigation Water Demand Sensitivity to Climate Variability Across the Contiguous United States. Water Resour. Res. 57, 1–16. https://doi.org/10.1029/ 2020WR027738.
- Nie, W., Kumar, S.V., Arsenault, K.R., Peters-Lidard, C.D., Mladenova, I.E., Bergaoui, K., Hazra, A., Zaitchik, B.F., Mahanama, S.P., McDonnell, R., Mocko, D.M., Navari, M., 2022. Towards effective drought monitoring in the Middle East and North Africa (MENA) region: implications from assimilating leaf area index and soil moisture into the Noah-MP land surface model for Morocco. Hydrol. Earth Syst. Sci. 26, 2365–2386. https://doi.org/10.5194/hess-26-2365-2022.
- Oleson, K.W., Lawrence, D.M., Bonan, G.B., Drewniak, B., Huang, M., Koven, C.D., Levis, S., Li, F., Riley, W.J., Subin, Z.M., Swenson, S.C., Thornton, P.E., Bozbiyik, A., Fisher, R., Heald, C.L., Kluzek, E., Lamarque, J.-F., Lawrence, P.J., Leung, L.R., Lipscomb, W., Muszala, S., Ricciuto, D.M., Sacks, W., Sun, Y., Tang, J., Yang, Z.-L., 2013. Technical Description of version 4.5 of the Community Land Model (CLM) NCAR/TN-503+STR.
- Ozdogan, M., Rodell, M., Beaudoing, H.K., Toll, D.L., 2010. Simulating the effects of irrigation over the united states in a land surface model based on satellite-derived agricultural data. J. Hydrometeorol. 11, 171–184. https://doi.org/10.1175/
- Pande, S., Savenije, H.H.G., Bastidas, L.A., Gosain, A.K., 2012. A Parsimonious Hydrological Model for a Data Scarce Dryland Region 909–926. https://doi.org/ 10.1007/s11269-011-9816-z
- Paniconi, Putti, M., 2015. Physically based modeling in catchment hydrology at 50: Survey and outlook. J. Am. Water Resour. Assoc. https://doi.org/doi:10.1002/ 2015WR017780
- Pinnington, E., Quaife, T., Black, E., 2018. Impact of remotely sensed soil moisture and precipitation on soil moisture prediction in a data assimilation system with the JULES land surface model. Hydrol. Earth Syst. Sci. 22, 2575–2588. https://doi.org/ 10.5194/hess-22-2575-2018.
- Pokhrel, Y., Hanasaki, N., Koirala, S., Cho, J., Yeh, P.J.F., Kim, H., Kanae, S., Oki, T., 2012. Incorporating anthropogenic water regulation modules into a land surface model. J. Hydrometeorol. 13, 255–269. https://doi.org/10.1175/JHM-D-11-013.1.
- Pokhrel, Y., Burbano, M., Roush, J., Kang, H., Sridhar, V., Hyndman, D.W., 2018a. A review of the integrated effects of changing climate, land use, and dams on Mekong river hydrology. Water (Switzerland) 10, 1–25. https://doi.org/10.3390/ w1030266
- Pokhrel, Y., Koirala, S., Yeh, P.J.-F., Hanasaki, N., Longuevergne, L., Kanae, S., Oki, T., 2014. Incorporation of groundwater pumping in a global Land Surface Model with the representation of human impacts 5375–5377. https://doi.org/10.1002/ 2013WR014979.Reply.
- Pokhrel, Y.N., Fan, Y., Miguez-Macho, G., Yeh, P.J.F., Han, S.C., 2013. The role of groundwater in the Amazon water cycle: 3. Influence on terrestrial water storage computations and comparison with GRACE. J. Geophys. Res. Atmos. 118, 3233–3244. https://doi.org/10.1002/jgrd.50335.
- Pokhrel, Y.N., Fan, Y., Miguez-Macho, G., 2014b. Potential hydrologic changes in the Amazon by the end of the 21st century and the groundwater buffer. Environ. Res. Lett. 9 https://doi.org/10.1088/1748-9326/9/8/084004.
- Pokhrel, Y.N., Koirala, S., Yeh, P.J.F., Hanasaki, N., Longuevergne, L., Kanae, S., Oki, T., 2015. Incorporation of groundwater pumping in a global Land Surface Model with the representation of human impacts. Water Resour. Res. 51, 78–96. https://doi.org/ 10.1002/2014WR015602.
- Pokhrel, Y.N., Hanasaki, N., Wada, Y., Kim, H., 2016. Recent progresses in incorporating human land-water management into global land surface models toward their integration into Earth system models. Wiley Interdiscip. Rev. Water 3, 548–574. https://doi.org/10.1002/wat2.1150.

- Pokhrel, Y., Shin, S., Lin, Z., Yamazaki, D., Qi, J., 2018b. Potential Disruption of Flood Dynamics in the Lower Mekong River Basin Due to Upstream Flow Regulation. Sci. Rep. 8, 1–13. https://doi.org/10.1038/s41598-018-35823-4.
- Portmann, F.T., Siebert, S., Döll, P., 2010. MIRCA2000-Global monthly irrigated and rainfed crop areas around the year 2000: A new high-resolution data set for agricultural and hydrological modeling. Global Biogeochem. Cycles 24, n/a-n/a. https://doi.org/10.1029/2008gb003435.
- Quichimbo, E.A., Singer, M.B., Michaelides, K., Hobley, D.E.J., Rosolem, R., 2021. a parsimonious hydrological model of DRYland Partitioning of the water balance DRYP 1. 0, 6893–6917.
- Reinecke, R., Müller Schmied, H., Trautmann, T., Seaby Andersen, L., Burek, P., Flörke, M., Gosling, S.N., Grillakis, M., Hanasaki, N., Koutroulis, A., Pokhrel, Y., Thiery, W., Wada, Y., Yusuke, S., Döll, P., 2021. Uncertainty of simulated groundwater recharge at different global warming levels: A global-scale multi-model ensemble study. Hydrol. Earth Syst. Sci. 25, 787–810. https://doi.org/10.5194/hess-25-787-2021.
- Rodell, M., Houser, P.R., Berg, A.A., Famiglietti, J.S., 2005. Evaluation of 10 methods for initializing a land surface model. J. Hydrometeorol. 6, 146–155. https://doi.org/ 10.1175/JHM414.1.
- Sakamoto, T., Van Phung, C., Kotera, A., Nguyen, K.D., Yokozawa, M., 2009. Analysis of rapid expansion of inland aquaculture and triple rice-cropping areas in a coastal area of the Vietnamese Mekong Delta using MODIS time-series imagery. Landsc. Urban Plan. 92, 34–46. https://doi.org/10.1016/j.landurbplan.2009.02.002.
- Save, H., Bettadpur, S., Center, B.D.T., 2016. High-resolution CSR GRACE RL05 mascons. AGU J. Geophys. Res. Solid Earth 119, 3076–3095. https://doi.org/10.1002/ 2016JB013007.Received.
- Scanlon, B.R., Faunt, C.C., Longuevergne, L., Reedy, R.C., Alley, W.M., McGuire, V.L., McMahon, P.B., 2012. Groundwater depletion and sustainability of irrigation in the US High Plains and Central Valley. Proc. Natl. Acad. Sci. U. S. A. 109, 9320–9325. https://doi.org/10.1073/pnas.1200311109.
- Shiklomanov, I.A., 2000. Appraisal and Assessment of world water resources. Water Int. 25, 11–32. https://doi.org/10.1080/02508060008686794.
- Shrestha, S., Bach, T.V., Pandey, V.P., 2016. Climate change impacts on groundwater resources in Mekong Delta under representative concentration pathways (RCPs) scenarios. Environ. Sci. Policy 61, 1–13. https://doi.org/10.1016/j. envsci.2016.03.010.
- Siebert, S., Döll, P., 2010. Quantifying blue and green virtual water contents in global crop production as well as potential production losses without irrigation. J. Hydrol. 384, 198–217. https://doi.org/10.1016/j.jhydrol.2009.07.031.
- Siebert, S., Kummu, M., Porkka, M., Döll, P., Ramankutty, N., Scanlon, B.R., 2015.
 A global data set of the extent of irrigated land from 1900 to 2005. Hydrol. Earth Syst. Sci. 19, 1521–1545. https://doi.org/10.5194/hess-19-1521-2015.
- Sivapalan, M., Jothityangkoon, C., Menabde, M., 2002. Linearity and nonlinearity of basin response as a function of scale: Discussion of alternative definitions 38, 1–5.
- Sophocleous, M., 2002. Interactions between groundwater and surface water: The state of the science. Hydrogeol. J. 10, 52–67. https://doi.org/10.1007/s10040-001-0170-8.
- Sun, C., Xiao, Z.N., Nguyen, M., 2021. Projection on precipitation frequency of different intensities and precipitation amount in the Lancang-Mekong River basin in the 21st century. Adv. Clim. Chang. Res. 12, 162–171. https://doi.org/10.1016/j. acre. 2021.03.001.
- Swenson, S.C., Clark, M., Fan, Y., Lawrence, D.M., Perket, J., 2019. Representing Intrahillslope Lateral Subsurface Flow in the Community Land Model. J. Adv. Model. Earth Syst. 11, 4044–4065. https://doi.org/10.1029/2019MS001833.

- Tatsumi, K., Yamashiki, Y., 2015. Effect of irrigation water withdrawals on water and energy balance in the Mekong River Basin using an improved VIC land surface model with fewer calibration parameters. Agric. Water Manag. 159, 92–106. https://doi.org/10.1016/j.agwat.2015.05.011.
- Tegegne, G., Park, D.K., Kim, Y., 2017. Journal of Hydrology: Regional Studies Comparison of hydrological models for the assessment of water resources in a data-scarce region, the Upper Blue Nile River Basin. J. Hydrol. Reg. Stud. 14, 49–66. https://doi.org/10.1016/j.ejrh.2017.10.002.
- Thompson, J.R., Green, A.J., Kingston, D.G., Gosling, S.N., 2013. Assessment of uncertainty in river flow projections for the Mekong River using multiple GCMs and hydrological models. J. Hydrol. 486, 1–30. https://doi.org/10.1016/j. ihydrol.2013.01.029.
- Tiwari, A.D., Pokhrel, Y., Kramer, D., Akhter, T., Lakshmi, V., Tang, Q., Liu, J., Qi, J., Loc, H.H., 2023. A synthesis of hydroclimatic, ecological, and socioeconomic data for transdisciplinary research in the Mekong 1–26. https://doi.org/10.1038/s41597-023-02193-0.
- Tran, D.A., Tsujimura, M., Pham, H.V., Nguyen, T.V., Ho, L.H., Le Vo, P., Ha, K.Q., Dang, T.D., Van Binh, D., Doan, Q.V., 2022. Intensified salinity intrusion in coastal aquifers due to groundwater overextraction: a case study in the Mekong Delta, Vietnam. Environ. Sci. Pollut. Res. 29, 8996–9010. https://doi.org/10.1007/s11356-021-16282-3
- Tu, T.A., Tweed, S., Dan, N.P., Descloitres, M., Quang, K.H., Nemery, J., Nguyen, A., Leblanc, M., Baduel, C., 2022. Localized recharge processes in the NE Mekong Delta and implications for groundwater quality. Sci. Total Environ. 845 https://doi.org/10.1016/j.scitotenv.2022.157118.
- Wada, Y., de Graaf, I.E.M., de G., Beek, L.P.H. van, 2016. High-resolution modeling of human and climate impacts on global water resources. J. Adv. Model. Earth Syst. 8, 1180–1209. https://doi.org/10.1002/2015MS000618.Received.
- Wada, Y., Van Beek, L.P.H., Van Kempen, C.M., Reckman, J.W.T.M., Vasak, S., Bierkens, M.F.P., 2010. Global depletion of groundwater resources. Geophys. Res. Lett. 37, 1–5. https://doi.org/10.1029/2010GL044571.
- Wada, Y., Wisser, D., Eisner, S., Flörke, M., Gerten, D., Haddeland, I., Hanasaki, N., Masaki, Y., Portmann, F.T., Stacke, T., Tessler, Z., Schewe, J., 2013. Multimodel projections and uncertainties of irrigation water demand under climate change. Geophys. Res. Lett. 40, 4626–4632. https://doi.org/10.1002/grl.50686.
- Watkins, M.M., Wiese, D.N., Yuan, D.-N., Boening, C., Landerer, F.W., 2014. Improved methods for observing Earth's time variable mass distribution with GRACE using spherical cap mascons Michael. AGU J. Geophys. Res. Solid Earth 119, 3076–3095. https://doi.org/10.1002/2014JB011547.Received.
- Weedon, G.P., Balsamo, G., Bellouin, N., Gomes, S., Best, M.J., Viterbo, P., 2014. Data methodology applied to ERA-Interim reanalysis data. Water Resour. Res. 50, 7505–7514. https://doi.org/10.1002/2014WR015638.Received.
- Wu, W., Clark, J.S., Vose, J.M., 2010. Assimilating multi-source uncertainties of a parsimonious conceptual hydrological model using hierarchical Bayesian modeling. J. Hydrol. 394, 436–446. https://doi.org/10.1016/j.jhydrol.2010.09.017.
- J. Hydrol. 394, 436–446. https://doi.org/10.1016/j.jhydrol.2010.09.017.
 Yeh, P.J.F., Eltahir, E.A.B., 2005. Representation of water table dynamics in a land surface scheme. Part II: Subgrid variability. J. Clim. 18, 1881–1901. https://doi.org/10.1175/JCJJ3331.1
- Zeng, Y., Xie, Z., Yu, Y., Liu, S., Wang, L., Zou, J., Qin, P., Jia, B., 2016. Effects of anthropogenic water regulation and groundwater lateral flow on land processes Yujin. J. Adv. Model. Earth Syst. 8 https://doi.org/10.1002/2016MS000646. Received.
- Zeng, Y., Xie, Z., Liu, S., Xie, J., Jia, B., Qin, P., Gao, J., 2018. Global Land Surface Modeling Including Lateral Groundwater Flow. J. Adv. Model. Earth Syst. 10, 1882–1900. https://doi.org/10.1029/2018MS001304.